

**ELECTROCARDIOGRAM SIGNAL PROCESSING  
USING  
JOINT TIME-FREQUENCY TOOLS**

*A Dissertation Submitted in Partial Fulfillment of the Requirements for the Award of  
the Degree of*

**MASTER OF ENGINEERING**

in

**Electronics and Communication Engineering**

Submitted by

**ADITI BAJAJ**

801561002

Under Supervision of

**Dr. Sanjay Kumar**

Associate Professor, ECED



**ELECTRONICS AND COMMUNICATION ENGINEERING DEPARTMENT  
THAPAR UNIVERSITY PATIALA, PUNJAB  
JULY 2017**



# DECLARATION

I, **Aditi Bajaj** hereby declare that the work presented in this thesis entitled **Electrocardiogram Signal Processing using Joint Time-Frequency Tools**, in partial fulfillment of the requirement for the award of degree of Master of Engineering submitted at Electronics and Communication Engineering Department, Thapar University, Patiala is an authentic record of work carried out under supervision of **Dr. Sanjay Kumar** (Associate Professor, ECED, Thapar University, Patiala). The matter presented in this has not been submitted either in part or full to any other university or institute for the award of any other degree.

Date: 5/9/17



---

**ADITI BAJAJ**

REG No.801561002

It is certified that the above statement made by the candidate is correct to the best of my knowledge and belief.

Date: 5/9/17



---

**Dr. Sanjay Kumar**

Associate Professor

ECED, TU, Patiala



*Matr devo bhava*

*Pitr devo Bhava*

*Acharya devo bhava*

Look upon your mother as your God

Look upon your father as your God

Look upon your teacher as your God

- from the sacred Vedic hymns of the Taittireeya Upanishad of India



# ACKNOWLEDGEMENT

It gives me great pleasure to find an opportunity to express my deep gratitude and sincerest thank to my guide Dr. Sanjay Kumar (Associate Professor) ECED, Thapar University, Patiala for giving most valuable suggestion, helpful guidance and encouragement in the execution of this thesis work. His guidance and cooperation has led me to the successful completion of work. I am highly indebted to him for the way he modeled and structured my work with his valuable tips, and the suggestion that he accorded to me in every aspect of my work.

I am also thankful to our Head of the Department, Dr. Alpana Agarwal for providing me adequate environment in carrying the thesis work. I would also like to thank Dr. Prashant Rana, CSED, Thapar University, Patiala for giving his valuable time to teach me everything I know about LATEX. It is due to him i am able to write my thesis in latex.

I would also like to give special acknowledgement to my fellow mate Amandeep Kaur for her support. Many thanks to my friends Yashjeet Kaur, Mehndi Goyal, Ayuk Mahajan, Abhinav Kapila and my ECE classmates for their unfailing support, wishes and continuous encouragement for the successful completion of thesis.

I would also like to acknowledge the Department of Science and Technology (DST) for making me the part of the research project sanctioned by Science and Engineering Research Board (SERB) and providing all the required support.

Last but not the least, I would like to thank my family: my parents, my grandmother and brother for supporting me spiritually through writing of this thesis and my life in general.

Above all I thank the Almighty God for being my strength and showering his blessings and grace towards me in all walks of my life.

**ADITI BAJAJ**



# ABSTRACT

Electrocardiogram (ECG), is a non-invasive technique which is used as a primary tool to diagnose cardiovascular diseases. ECG is non-stationary signal, so it cannot give good time or frequency resolution, as it is well established by the research communities that the Fourier transform is not the most viable tool for the time-frequency signal analysis and processing. So joint time-frequency analysis(JTFA) tools are introduced to get more accurate results in the non-stationary signal environment.

JTFA Techniques like Short-time Fourier transform, Wigner-Ville distribution, Wavelet transform, and S-transform are discussed and contrasted to overcome the drawbacks of Fourier transform. Different parameters that make S-transform better than other transforms have been discussed.

We will exploit the advantages of the S-transform to denoise the ECG signal, and for isolating the QRS complexes in the time- frequency domain. Concept of Shannon energy is introduced and applied, instead of classical squared energy to get significant amplitude changes of QRS and to emphasis medium and low QRS beats.

The work presented in this thesis mainly focuses on to investigate application of JTFA tool on ECG signal. Qualitative measures like Root Mean Square Error(RMSE), Signal to Noise Ratio(SNR), Sensitivity, Positive Predictivity etc. are used for validating the results obtained for denoising and QRS detection. ECG data is taken from the standard database of MIT-BIH arrhythmia database. A modified variant of S-transform in fractional frequency domain is also proposed for biomedical signal processing.

The main objective is to predict JTFA tools valuable in the biomedical field so that future developments in this field can come up.



# TABLE OF CONTENTS

Sr. No.	Title	Page No.
<b>Declaration</b>		<b>i</b>
<b>Acknowledgement</b>		<b>v</b>
<b>Abstract</b>		<b>vii</b>
<b>LIST OF FIGURES</b>		<b>xi</b>
<b>LIST OF TABLES</b>		<b>xiii</b>
<b>Chapter 1 INTRODUCTION</b>		<b>1</b>
1.1	General	1
1.2	Shortcomings of Fourier Transform	2
1.3	Fundamentals of Uncertainty Principle	2
1.4	Motivation behind Joint Time-Frequency Analysis	3
1.4.1	Linear Representation	4
1.4.1.1	Gabor transform	4
1.4.1.2	Short Time Fourier Transform	5
1.4.1.3	Wavelet Transform	5
1.4.2	Quadratic Representation	7
1.4.2.1	Wigner-Ville Distribution	7
1.4.2.2	Cohen class of distribution	8
1.5	Stockwell Transform	8
1.6	Fractional S-transform	8
1.7	Biomedical signals	9
1.8	Organization of Thesis	10
<b>Chapter 2 LITERATURE SURVEY</b>		<b>11</b>
2.1	Preliminaries of ST	11
2.2	Preliminaries of FrST	12
2.3	Preliminaries of ECG Denoising	12
2.4	Preliminaries of QRS Localisation and Shannon Energy	13
2.5	Preliminaries of QRS Detection	14

<b>Chapter 3 ECG Analysis in Time-Frequency Domain . . . . .</b>	<b>15</b>
3.1 Bioelectric Signal- Origin and Nature . . . . .	15
3.2 Heart Anatomy . . . . .	15
3.3 Heart's Electrical System . . . . .	16
3.4 Introduction to Electrocardiogram (ECG) . . . . .	17
3.4.1 Interpretation of ECG waveform . . . . .	18
3.5 Processing and Analysis of ECG . . . . .	20
3.5.1 ECG Electrode Placement and ECG Leads . . . . .	21
3.6 Noises in ECG . . . . .	23
3.7 Artifacts Removal . . . . .	24
3.8 Abnormalities in ECG . . . . .	25
3.9 S-transform . . . . .	26
3.9.1 Deduction from STFT and wavelet . . . . .	26
3.9.2 Inverse S-transform . . . . .	27
3.9.3 Discrete S-transform . . . . .	28
3.10 Fractional ST- A novel JTFA Tool . . . . .	29
3.10.1 Theoretical and Mathematical Background . . . . .	29
3.10.2 Deduction of FrST from ST and FrFT . . . . .	31
3.11 Uncertainty principle and FrST . . . . .	32
<b>Chapter 4 JOINT TIME-FREQUENCY ANALYSIS OF ECG . . . . .</b>	<b>35</b>
4.1 ECG denoising using ST . . . . .	35
4.1.1 Methodology . . . . .	36
4.2 Denoising using FrST . . . . .	39
4.2.1 Proposed Methodology . . . . .	40
4.3 Performance Metric . . . . .	42
4.4 Results and Discussions . . . . .	43
4.5 QRS Detection using T-F method . . . . .	46
4.5.1 Concept of Shannon energy and QRS localization . . . . .	49
4.5.2 QRS detection using ST . . . . .	50
4.5.3 QRS detection using FrST . . . . .	50
4.5.4 Results and Discussion . . . . .	51
<b>Chapter 5 CONCLUSION AND FUTURE SCOPE OF WORK . . . . .</b>	<b>59</b>
5.1 Conclusion . . . . .	59
5.2 Future Scope . . . . .	60
<b>References . . . . .</b>	<b>61</b>

# LIST OF FIGURES

Sr.No.	Figure Details	Page No.
Figure 1.1	Types of time-frequency distributions . . . . .	3
Figure 1.2	STFT Analysis [3] . . . . .	5
Figure 1.3	Time scale analysis [3] . . . . .	6
Figure 1.4	Time based, frequency based and STFT views of signal [3] . . . . .	6
Figure 3.1	Structure of heart representing chambers, valves, vessels and conduction system of heart . . . . .	16
Figure 3.2	Electrical system of the heart . . . . .	17
Figure 3.3	Schematic of normal sinus rhythm for a heart as seen on ECG [8] . . . . .	18
Figure 3.4	Biomedical signal processing and analysis [8] . . . . .	21
Figure 3.5	Einthoven's triangle . . . . .	22
Figure 3.6	ECG signal and ST spectrum . . . . .	27
Figure 3.7	Implementation of Discrete ST . . . . .	28
Figure 3.8	Time and fractional fourier frequency domain plane . . . . .	30
Figure 3.9	ECG signal and FrST spectrum . . . . .	32
Figure 3.10	Compact support set of signal in time-frequency plane . . . . .	33
Figure 3.11	Compact support set for signal with optimal order . . . . .	33
Figure 4.1	Block diagram for ECG denoising method ST . . . . .	36
Figure 4.2	Flowchart for calculating Discrete ST [31] . . . . .	37
Figure 4.3	ST of a noisy ECG record 119 . . . . .	38
Figure 4.4	T-f distribution of noisy ECG record 119 after masking . . . . .	38
Figure 4.5	T-f distribution obtained after thresholding and filtering . . . . .	39
Figure 4.6	Denoised ECG signal . . . . .	39
Figure 4.7	Block diagram for proposed ECG denoising method . . . . .	40
Figure 4.8	Time-fractional frequency domain representation of ECG signal record 119 . . . . .	40
Figure 4.9	Time-fractional frequency domain representation after masking . . . . .	41
Figure 4.10	Time-fractional frequency domain representation after thresholding . . . . .	41
Figure 4.11	Filtering done without rotation and with rotation of signal . . . . .	42
Figure 4.12	Comparison of the PRD(%) using different denoising methods . . . . .	48

Figure 4.13	Normalized energy values with Shannon energy (solid) and squared energy (dashed)[21]. . . . .	49
Figure 4.14	a) ECG-214 b)ST spectrum c) Shannon energy plot . . . . .	52
Figure 4.15	a) ECG-214 b) FrST spectrum c) Shannon energy plot . . . . .	52
Figure 4.16	a) ECG-117 b) ST spectrum c) Shannon energy plot . . . . .	53
Figure 4.17	a) ECG-117 b) FrST spectrum c) Shannon energy plot . . . . .	53
Figure 4.18	a) ECG-208 b) ST spectrum c) Shannon energy plot . . . . .	54
Figure 4.19	a) ECG-208 b) FrST spectrum c) Shannon energy plot . . . . .	54

# LIST OF TABLES

Sr.No.	Table Details	Page No.
Table 3.1	Normal ECG's Amplitudes and Duration [8] . . . . .	19
Table 3.2	Abnormality in ECG [13] . . . . .	25
Table 4.1	Performance results for ST based Denoising without added noise . .	43
Table 4.2	Performance results for ST based Denoising with added noise . . . .	44
Table 4.3	FrST based denoising without added noise with a=0.4, p=0.511, q= 0.51 . . . . .	44
Table 4.4	FrST based denoising with added noise with a=0.4, p=0.511, q= 0.51 . . . . .	45
Table 4.5	FrST based denoising without added noise with a=0.5, p=0.511, q= 0.51 . . . . .	45
Table 4.6	FrST based denoising with added noise with a=0.5, p=0.511, q= 0.51 . . . . .	46
Table 4.7	FrST based denoising without added noise with a=0.6, p=0.511, q= 0.51 . . . . .	46
Table 4.8	FrST based denoising with added noise with a=0.6, p=0.511, q= 0.51 . . . . .	47
Table 4.9	FrST based denoising without added noise with a=0.3, p=0.511, q= 0.51 . . . . .	47
Table 4.10	FrST based denoising with added noise with a=0.3, p=0.511, q= 0.51 . . . . .	48
Table 4.11	Comparison of the algorithms . . . . .	55
Table 4.12	Experimental results for QRS detection using ST . . . . .	56
Table 4.13	Experimental results for QRS detection using FrST . . . . .	57



# Chapter 1

## INTRODUCTION

### 1.1 General

A signal which is non-stationary is a stochastic signal, whose statistical structure varies with respect to time, e.g., the mean, variance, correlation (covariance), etc., change as time changes. Non-random signals may show a non-stationary form examples being a chirp signal, for which we could refer to, a “changing frequency”. The phenomena exhibit non-stationarity[1]. These signals have variable power spectra dependent on frequency but frequency content of the most signals in real world evolves time and the traditional power spectrum does not reveal much important information.

To overcome the problem, many time-frequency tools such as short-time fourier transform (STFT), continuous wavelet transform (CWT), Gabor expansion and Wigner-Ville distribution (WVD) have been developed. Thus Time-Frequency Signal analysis and Processing(TFSAP) concerns the analysis and processing of signals with time-varying frequency content. So basically TFSAP is a collaboration of theory employed for analysis and processing of non-stationary signals, which can be found in a very vast range of fields like seismology and biomedical engineering.

The S-transform(ST) is a new time-frequency method introduced by Stockwell [2], which suitably amalgamate the strengths of the STFT and wavelet transforms (WT). Therefore, it provides extra details about spectra which is not available with the continuous wavelet transform. The ST is being used in various fields such as geophysics, biomedical engineering, power transformer protection, power quality analysis, oceanography, atmospheric physics, medicine, hydrogeology and mechanical engineering. Its performance is much better than traditional time-frequency methods. In the field of biomedical engineering, ST had been used for the analyzing cardiac abnormalities signals, EEG recordings analysis in epilepsy patients and identification of abnormalities in brain tumors.

## 1.2 Shortcomings of Fourier Transform

Frequency and time are two basic variables of signal analysis and processing. The Fourier Transform (FT), providing a mapping between the time domain and frequency domain representations of a signal, can be considered as a reformulation of the time domain signal with respect to the frequency variable along with complex sinusoidal exponentials [3]. The continuous time FT  $S(f)$  of a time domain signal is defined as:

$$S(f) = \int_{-\infty}^{+\infty} s(t) e^{-j2\pi ft} \quad (1.1)$$

where  $s(t)$  is a signal, whose FT is being calculated.

FT is the most popular transform used for stationary signals, which has time independent power spectra. FT shows which frequency components are present in a signal. But problem in this classical representations is its non-localization [4] with respect to the excluded variable. In case of stationary signals, time-frequency domain representations are appropriate but these classical representations fail in case of non-stationary signals. FT has the following Limitations [5]:

1. Simultaneous time and frequency localization cannot be provided.
2. Not very useful in analyzing time-variant signals.
3. Not appropriate for representing discontinuities.
4. What frequencies are present in the signal can be known from the magnitude spectrum, but times of arrival of those frequencies cannot be known.

Many applications are based on determining the frequency content of the signal. Although FT is an important signal analysis tool, but various other related transforms are being formulated to address the shortcomings of FT.

## 1.3 Fundamentals of Uncertainty Principle

Decomposition of a time domain signal into frequency domain is given by fourier analysis. So by introducing both time and frequency simultaneously into the picture, one can see when does frequency component make its dominant contribution in signal  $x(t)$ . Indeed,

this seems to be very illusional when *Uncertainty Principle* [4] is considered. Principle is brievely summarized as,

$$\Delta\omega\Delta t \geq \frac{1}{2} \tag{1.2}$$

where time width ( $\Delta t$ ) signifies how well two spikes in time can be separated from each other in the frequency domain and bandwidth ( $\Delta\Omega$ ) signifies how well two spectral components can be separated from each other in the time domain. This is also called as Bandwidth-Time product (BT product) [4]. In other words, this principle tells that more precisely one specifies 'when' for a signal, the less accurately can one specify the involved frequencies.

## 1.4 Motivation behind Joint Time-Frequency Analysis

In non-stationary signal processing field, the time-frequency transform is an important tool. The FT only maps the signal from one-dimensional time domain to one-dimensional frequency domain. After the transformation, although the signal has a very good frequency resolution, but the time resolution is lost completely. This is not acceptable for non-stationary signal processing. Therefore the need arises for time-frequency analyses. Different distributions are shown in Figure 1.1.

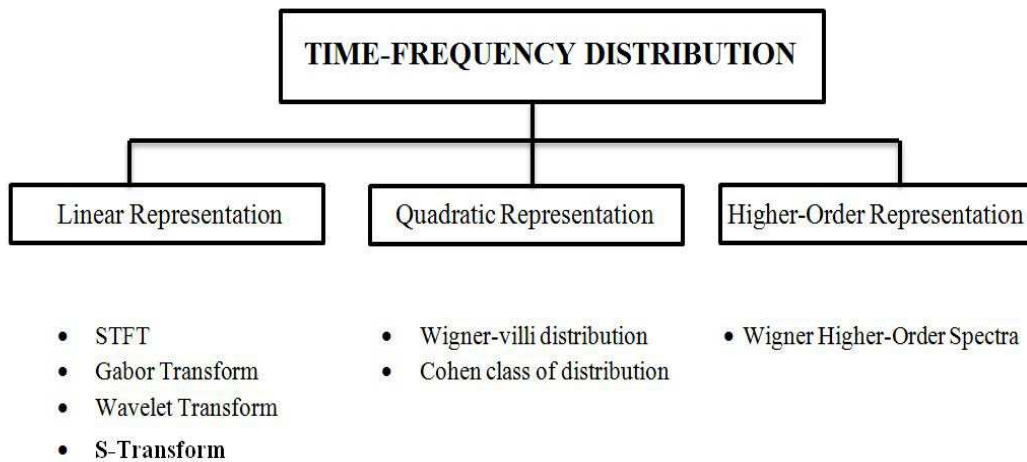


Figure 1.1: Types of time-frequency distributions

The method of time-frequency analyses converses the signal from time domain to time-frequency domain and non-stationary can be analysed to much greater extent. By use of window functions, tools [3] like short time fourier transform, wavelet transform

can overcome the disadvantages of the FT and enable us to study the time-frequency characteristics of signals which shows transient oscillatory behavior.

In the continuous domain, the accuracy limit is well-established by the Heisenberg's uncertainty [4] principle which has been presented in previous section, where the spread in time-frequency is measured in terms of variance. Decomposition of a function when time perspective is required in addition to information about frequency content is called time-frequency analysis.

## 1.4.1 Linear Representation

In this section the idea of representing a signal in terms of a set of other components is presented. Fourier series is one such example which on decomposing into components, adds back to the give the original signal. We will include related discussions to both deterministic and stochastic signals, for which the meaning of non-stationary concept is that we must modify the Fourier form in some way and yet we still wish the concept of frequency to be retained.

### 1.4.1.1 Gabor transform

In 1946, Gabor [6] noted that  $(t, f)$  plane can be split up into an array of rectangles and array dimension should satisfy the Heisenberg's uncertainty principle mentioned in Section 1.3. Gabor [3] considered representation of all signals (stochastic as well as stationary) in terms of sines and cosines modulated Gaussian pulse given by the form,

$$w_{n\Delta, \omega_k} = w(t - n\Delta) e^{j\omega_k t} \quad (1.3)$$

where  $w(t)$  are the Gaussian pulses. These basic elements have lowest BT product because only Gaussian pulse obeys the minimum condition of the (1.2). The signal  $x(t)$  was assumed to be summation of these modulated pulses i.e.,

$$x(t) = \sum_n \sum_k c_{nk} w(t - n\Delta) e^{j\omega_k t} \quad (1.4)$$

where the index  $n$  signifies the positions of the time pulse and the index  $k$  signifies the frequency. The coefficients are spread over the time-frequency plane. The representation in (1.4) is discrete in "cells" over time and frequency integral representations for continuous case. Also, Gabor representation can be assumed as a sampled version of STFT.

### 1.4.1.2 Short Time Fourier Transform

To overcome the shortcomings of the FT, it was necessary to instigate a window of predetermined length which slides through the signal along the axis of time to perform a “time-localized” FT. This concept led to the Short-Time Fourier Transform (STFT) [7], introduced by Dennis Gabor (1946). The STFT can be expressed as:

$$STFT(\tau, f) = \langle x, g_{\tau, f} \rangle = \int x(t) g(t - \tau) e^{-j2\pi ft} dt \quad (1.5)$$

where  $\langle \cdot, \cdot \rangle$  signifies the inner product between signal  $x$  and window  $g$ , with  $t$  as time location parameter and  $f$  as frequency parameter. In this, only a small section of Fourier transform is analyzed at a time – a technique called windowing the signal. STFT maps a signal into a two-dimensional function of time and frequency.

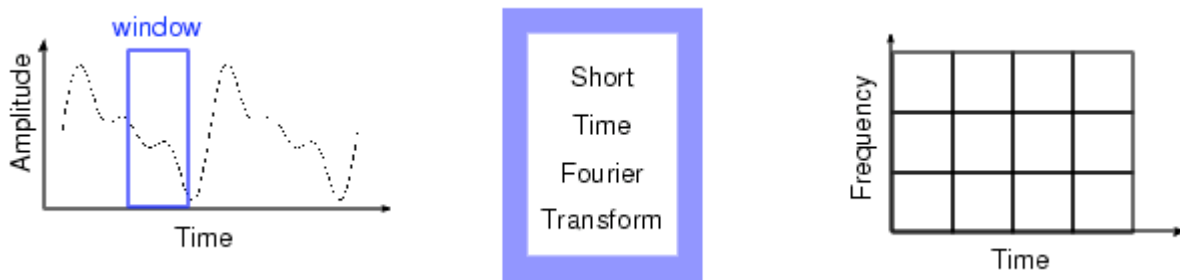


Figure 1.2: STFT Analysis [3]

The STFT provides a kind of trade off between the time and frequency based views of a signal. It gives some information about the both, time of occurrence and at what frequencies it occurs but with limited precision, and this precision is given by the size of the window. While this trade off between time and frequency information can be useful, the drawback is that the size of window once chosen is then fixed for all frequencies. A more flexible approach is needed for many signals i.e., where the window size can be changed to estimate either time or frequency accurately.

### 1.4.1.3 Wavelet Transform

The next logical step is wavelet analysis i.e., it’s variable sized windowing technique. The wavelet transform [8] has variable sized windows for different frequency components within a signal. This is realized by comparing the signal with a set of template functions obtained from the scaling (i.e., dilation and contraction) and shift (i.e., translation along



Figure 1.3: Time scale analysis [3]

the time axis) of a mother wavelet and looking for their similarities. The notation of inner product for the wavelet transform of a signal  $x(t)$  can be expressed as,

$$wt(s, \tau) = \langle x, \psi_{s, \tau} \rangle = \frac{1}{\sqrt{s}} \int_{-\infty}^{+\infty} x(t) \psi * \left( \frac{t - \tau}{s} \right) dt \quad (1.6)$$

where  $x$  is the signal,  $\psi$  is the wavelet,  $\tau$  is the time location parameter, and  $s$  is the scale parameter and  $t$  is the time.

The use of long time intervals is allowed by the wavelet technique where more precise low frequency information is needed, and shorter regions where high frequency information is required. Time-frequency region is not used by the wavelet technique but time scale region is used. We have discussed various transforms and starting with the

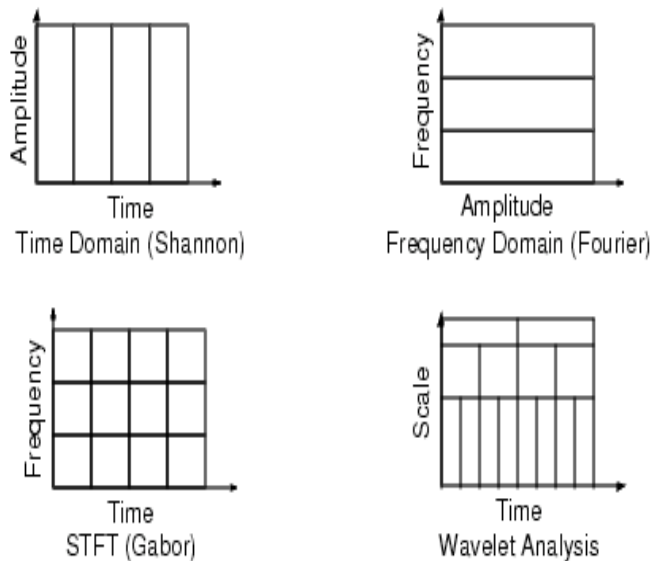


Figure 1.4: Time based, frequency based and STFT views of signal [3]

classical representations i.e., time and frequency domain (FT), so here is the time based,

frequency based and STFT views of a signal.

## 1.4.2 Quadratic Representation

This section is referred to as quadratic representation [1] or “energetic” view on time-frequency methods. STFT and WT allow signal energy to be displayed in time-frequency  $(t, \omega)$  or in time-scale plane i.e., for the spectrogram,

$$\frac{1}{2\pi} \iint |S(t, \omega)|^2 dt d\omega = E_x = \int |x(t)|^2 dt \quad (1.7)$$

and for the scalogram,

$$\iint |W(t, s)|^2 \frac{dt da}{s^2} = E_x \quad (1.8)$$

Both STFT [3] and WT [6] follow linear representation of the signal which allow the signal’s energy to be displayed in the  $(t, \omega)$  or  $(t, s)$  plane.

### 1.4.2.1 Wigner-Ville Distribution

The WVD [3] of a signal  $x(t)$  is defined in time domain as:

$$W_x(t, \omega) = \int_{-\infty}^{+\infty} x\left(t + \frac{\tau}{2}\right) x^*\left(t - \frac{\tau}{2}\right) e^{-j\omega\tau} d\tau \quad (1.9)$$

where  $x^*(t)$  is the complex conjugate of  $x(t)$ . In the frequency domain, WVD is defined as follows:

$$W_x(t, \omega) = \int_{-\infty}^{+\infty} X\left(\omega + \frac{\zeta}{2}\right) X^*\left(\omega - \frac{\zeta}{2}\right) e^{j\zeta t} d\zeta \quad (1.10)$$

where  $X(\omega)$  is the Fourier transform of  $x(t)$ . Various intended properties of the WVD [1] are time preservation and support of frequency, infinite time and frequency resolution etc., makes WVD a useful tool for signal analysis. The main demerit of this distribution is the fact that it is quadratic and it introduces cross terms in the time-frequency domain. These cross-terms [8] are undesired and can be reduced by applying low-pass filter to WVD [9]. The smoothing, however, will decrease the resolution of frequency of the WVD and cause the loss of some useful transformation properties.

### 1.4.2.2 Cohen class of distribution

Cohen generalized the definition in such a way that this class includes a wide variety of distributions. The generalized function: i.e.,

$$S_g(t, \omega) = \int R(t, \tau) e^{-j\omega\tau} d\tau = \iint g(u - t, \tau) x * \left(u - \frac{\tau}{2}\right) x \left(u + \frac{\tau}{2}\right) e^{-j\omega\tau} d\tau du \quad (1.11)$$

where the function  $g(t, \tau)$  is the kernel function [9], choice of which defines the different distributions.

## 1.5 Stockwell Transform

Stockwell Transform (ST) is a time-frequency analysis tool which combines the properties of the both, STFT and wavelet transform. It provides resolution dependent frequency sustaining a direct relationship with the Fourier spectrum. It is an extension of the short-time Fourier transform ideas and is based on a moving and scalable localizing Gaussian [10] window.

$$S(\tau, f) = \int_{-\infty}^{+\infty} x(t) \omega(\tau - t) e^{-j2\pi ft} dt \quad (1.12)$$

where  $x(t)$  is the signal and  $\omega(t)$  is the scalable Gaussian window function.

## 1.6 Fractional S-transform

Fractional S-transform (FrST) is a latest Fractional Time-Frequency Analysis tool, which is based on the idea of adopting the fractional fourier transform(FRFT) [10] kernel instead of FT kernel just like in existing time-frequency transforms. So FrST is simply, the extension of ST from time-frequency domain to time-fractional frequency domain. For a signal  $x(t)$ , an  $a^{th}$  order FrST [11] is defined as:

$$FrST_x^a(\tau, u) = \int_{-\infty}^{+\infty} x(t) g(\tau - t, u) K_a(t, u) dt \quad (1.13)$$

where  $K_a(t, u)$  is the kernel of the FRFT,  $g(\tau - t, u)$  is the Gauss function about  $t$  and  $u$  is the fractional fourier frequency [12].

## 1.7 Biomedical signals

Any signal which is intercepted from a biological or medical source is called a bio-signal. The molecule level, cell level, or a systemic or organ level can be its source. A wide variety of such signals are commonly encountered in the clinic, research laboratory, and sometimes even at home. Electrocardiogram (ECG), or electrical activity from the heart; speech signals; the electroencephalogram (EEG), or electrical activity from the brain; evoked potentials (EPs, i.e., auditory, visual, somatosensory, etc.), or electrical responses of the brain to specific peripheral stimulation; action potential signals from individual neurons or heart cells; the electromyogram (EMG) [13], or electrical activity from the muscle; the electro-retino gram from the eye; are some of the examples.

Our analysis revolves around the ECG (electrocardiogram) signal. The ECG, which is nothing but recording of heart's electrical activity, provides important information about the varieties of Cardiac disorders depending upon the deviations from normal ECG signal pattern. In general, the frequency range of an ECG signal varies between 0.05-100 Hz with the dynamic range [12] between 1-10mV. The ECG signal is identified by five peaks and valleys namely addressed by the letters P, Q, R, S, T. In some cases U-peak is also used. The QRS complex is the most substantial waveform within the electrocardiographic (ECG) signal, with normal duration from 0.06s to 0.1s.

The performance of ECG [13] analyzing system primarily depends on the accurate and reliable detection of the QRS complex, in addition to T-wave and P-wave. However, due to the time-varying morphology [14] of the QRS complexes, they are not always the strongest signal component in an ECG signal. In addition there are many sources of noise in a clinical environment, for example, power line interference, muscle contraction noise, poor electrode contact, patient movement, and baseline wandering; which is due to respiration, can degrade the ECG signal. The electrocardiogram (ECG) is an important tool for providing information about functional status of the heart.

The correct performance of analyzing system depends on many vital factors, including the quality of the ECG signal, the applied classification rule, and also on learning and testing data set. The ECG is characterized by a recurrent wave sequence of P, QRS and T wave associated with each beat. The QRS complex is the most appealing waveform which is caused by ventricular depolarization of the heart. Once the QRS complexes positions are found, the locations of other components of ECG like P, T waves and ST [13] segment etc. can be determined, for analyzing the complete cardiac period.

The QRS complex is a name for the combination of three of the graphical deflections seen on a typical electrocardiogram (EKG or ECG). It is often the central and most visually prominent part of the tracing. It relates to the depolarization of the right and left ventricles of the human heart. The Q, R, and S waves occur in quick succession, also they do not appear all in all leads, and emit a single event, and thus are usually considered together.

## 1.8 Organization of Thesis

The thesis is organized into 5 chapters. A brief outline is given below:

- **Chapter 1** This chapter briefly reviewed the existing time-frequency methods and about biomedical signals.
- **Chapter 2** This section presents the literature review for the research work. It presents the preliminaries of ST, FrST, shannon energy , denoising and QRS detection.
- **Chapter 3** This sections briefly gives the description of human heart and its working. Summarises of the steps involved in processing of ECG, mentioning about various noises and their removal techniques is also mentioned. It introduces the new approach of JTFA method.
- **Chapter 4** This chapter gives the detailed description about the work that was carried out during research work. Denoising and QRS detection using JTFA methods is discussed and their performance is described using graphs and various statistical parameters.
- **Chapter 5:** Finally, the conclusion of study with future scope of the work is presented and discussed in this chapter.

# Chapter 2

## LITERATURE SURVEY

*Research is what I'm doing when I don't know what I'm doing.- Werner von Braun*

A thorough and substantial literature review highlights one's credibility in his field and is the key for successful research. In other words, "Literature Review" is a re-organization of the information in a way that shows our planning to work upon a research problem. This chapter outlines the study done for thesis. Also, it presents the objectives to carry out the thesis work and literature reviewed for the work presented in thesis.

### 2.1 Preliminaries of ST

Stockwell *et al.* [2] proposed the concise introduction to the concept of ST, which is known for its locally referenced phase properties. In this paper more efficient representation is introduced as a orthogonal set of basis functions, which localizes the spectrum and retains the advantageous phase properties of the ST. This approach allows one to measure phase shifts by performing localized cross spectral analysis. It is measured between multiple components of two time series as a function of both frequency and time.

Ventosa *et al.* [5] addresses the simplicity of ST, to work well in only continuous domain and mentions limitations of ST in discrete domain. This paper compares ST with better known continuous wavelet transform (CWT). Wavelet reconstruction formula is employed as a formula for inverse ST. Many methods are proposed to resolve the problems of discrete ST.

Daubechies *et al.* [6] explains the development of wavelets, emerged from the ideas of many different fields, which are combined to merge as a whole. New applications could be described which would not have been possible if this merging had not taken place.

Sahu *et al.* [7] proposed a modified Gaussian window to improve energy concentration of ST. The window is efficiently scaled with frequency. The proposed method is proved to have potential for analysing variety of test signals. Results in the study revealed that by using modified gaussian window, better time-frequency localization is achieved.

Stockwell *et al.* [9] mentioned the absence of CWT to have desirable characteristics. Unique feature of ST which is to provide frequency-dependent resolution, results in maintaining a direct relationship with the Fourier spectrum. These advantages of the ST are due to the fact that localised scalable Gaussian window translates as well as dilates, whereas modulating sinusoids are fixed with respect to the time axis.

## 2.2 Preliminaries of FrST

Ping *et al.* [11] introduced a novel method based on the combination of FrFT and ST. FrST is said to enhance the ability for analysing the spectrum of the signal. He proposed new method of processing transient signals.

Wang *et al.* [12] extended the concept of time-bandwidth product to fractional frequency domain. He introduced the method to find optimal order of FrST which is based on the calculation of normalized second-order central moment. Proposed algorithm showed better time-frequency concentration, producing more compact time-frequency support than the ST.

## 2.3 Preliminaries of ECG Denoising

Chandrakar *et al.* [14] presented different artifacts, which get embedded to ECG signal and abrupt the original signal. Therefore digital filter are required for removing artifacts from the original signal are proposed.

Mahamdy *et al.* [15] presented five denoising methods and applied them on real ECG signals, contaminated with different noise levels. These algorithms are: discrete wavelet transform (universal and local thresholding), adaptive filters (LMS and RLS), and Savitzky-Golay filtering. Finally denoising performances of these algorithms are implemented and compared.

Sanyal *et al.* [16] used ST to eliminate baseline wander in ECG signals. Also, comparison

between the proposed approach and WT based method is established.

Khaing *et al.* [17] introduced an effective software based application to eliminate noises from the ECG signals. Digital filters based on such application are designed, implemented and tested, and their quantitative analysis is investigated. Also performance comparison between filtered noisy signal and original database ECG recordings is done by analysing power spectra and mean square error.

Agrawal *et al.* [18] stated that the key feature of ST, is to have simultaneous frequency resolution and referenced local phase. The non-stationary signal is processed using ST based filter.

## 2.4 Preliminaries of QRS Localisation and Shannon Energy

Manikandan *et al.* [19] presented a technique based on automated peak finding logic. Concept of Shannon energy envelope is utilised to detect R-peaks. This method along with the proposed preprocessor achieved high accuracy for finding wide, small and sudden changes in QRS.

Zhu *et al.* [21] introduced novel concept of detection of R-peak based on shannon energy envelope. Algorithm first extracts shannon energy envelope from ECG and then finds R-peaks using 3 sub-processes (peak detection, false-R detection and false-noise detection). This can avoid asystole case or long pause case segmentation of ECG.

Fonseca *et al.* [22] proposed a novel method for QRS localisation based on the R-wave slope detection. Also this method is said to give precise localisation regardless of QRS detector used.

Moukadem *et al.* [23] presented a new technique based on ST for heart sounds segmentation. This method segments the Phono-Cardio-Gram (PCG) signal. SSE method is applied to optimise the energy concentration by using a window width optimization algorithm.

## 2.5 Preliminaries of QRS Detection

Chen *et al.* [25] structured a computing method based on the concept of moving average filter. Detection algorithm also incorporates the wavelet denoising procedure which allows a high time and memory efficiency.

Hamilton *et al.* [26] investigated quantitative effects of common elements of QRS detection rules. Decision rule section in the preprocess which is to determine the QRS from noise was optimized. Thus a more complex decision process was developed to detect QRS.

Tompkins *et al.* [27] discussed a real-time algorithm for detecting QRS complex of ECG signals. Digital bandpass filter is presented, which is capable of reducing false detections caused by noise. This filtering allows the use of low thresholds, thereby increasing detection sensitivity. Meyer *et al.* [28] suggested an approach to automatically merge different QRS complex detection algorithms. Data driven parameters that will balance the contribution of individual algorithm are determined.

Zidelmal *et al.* [29] examined the method based on power spectrum using wavelet coefficients to analyse the QRS morphologies accurately.

Arzeno *et al.* [30] had presented the algorithms based on differentiated ECG which are computationally efficient. QRS detection is done using first-derivative and Hilbert transform (HT).

Alvarez *et al.* [32] compared three of the best QRS detection algorithms for getting better accuracy and performance. In addition, software is developed in order to allow test newly added QRS detection algorithms over different databases.

Rufas *et al.* [33] presented a new filtering method to detect QRS signal for less computational cost and resources. Present methods having high computational complexity and they require more resources for its implementation. Disadvantages of the existing methods are eliminated from the novel non-linear filter presented in this paper.

Yeh *et al.* [34] proposed Difference Operation Method (DOM) for detection of QRS complex of ECG signal. This method comprises of 2 stages. Firstly, difference equation operation is applied to find point R. The second stage is find position of points Q and S.

# Chapter 3

## ECG Analysis in Time-Frequency Domain

### 3.1 Bioelectric Signal- Origin and Nature

Concept of bio-electrical signal introduced by Galvani initiated the use electric simulation diagnosing diseases. Potential difference accumulated because of movement of ions in muscles and nerves give rise to this bio-electric signal [8] and amplitude of few microvolt is recorded.

### 3.2 Heart Anatomy

The heart is the apex organ of cardiovascular system and its location is in between lungs in the thoracic sternum cavity and it pumps the blood to body's each part. Its weight is about 0.45% of men's body weight and 0.40% in women.

The heart is a four chambered pump with two atriums and two ventricles, which are there for assimilating blood and rushing it out. The right atrium collects the impure blood coming from the body parts via superior and inferior vena cavae. While during the atrial contraction, blood is passed through tricuspid valve to reach the right ventricle from right atrium and during the ventricular systole the impure blood present in right ventricle is pumped out from lung for purification through pulmonary valve. This blood then goes back to the heart from left atrium passing from left ventricle, where it is pumped again for the distribution to the whole body through arteries.

The left atrium ventricle is biggest and highly important cardiac chamber which receives purified blood from the lungs, passes onto the ventricle through mitral valve during atrial contraction to the ventricle [13]. The two phases involved in cardiac cycle

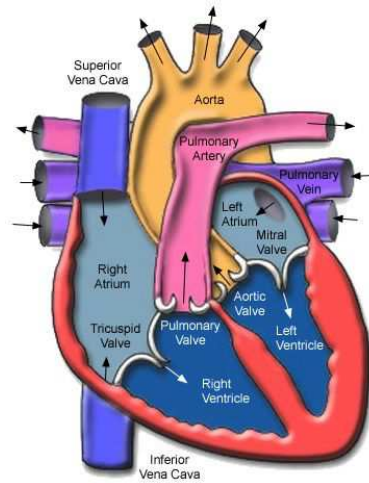


Figure 3.1: Structure of heart representing chambers, valves, vessels and conduction system of heart

of heart are termed as systole and diastole. The phase of pump or contract of cardiac chamber is called systole and the resting and filling phase of cardiac chamber is called diastole. Structure of heart is shown in Figure 3.1.

### 3.3 Heart's Electrical System

System of conduction and heart's electric events are special as well as synchronised, which plays huge role in activity of heart related to contraction which is rhythmic in nature. The electrical system of heart is made up of:

1. Sinoatrial(SA) Node, location is being in the hearts right atrium.
2. Atrioventricular(AV) node, location is near the tricuspid valve near interatrial septum
3. His-Purkinje system, location being at the terminals of left bundle branch and right bundle branch along the walls of heart's ventricles.

- Working of electrical system of human heart

Heart's electrical activity is mainly because of re-polarization and depolarization of myocardial cells. In rest mode, interior of cell membrane is more negative compared to outside and as an impulse electric in nature is generated, the interior part gets more positive with respect to the exterior part. This polarity change is called depolarisation.

After depolarisation original state of cell is restored. This is called re-polarisation. When heart muscle depolarize and re-polarize, ECG records the electrical signal [13].

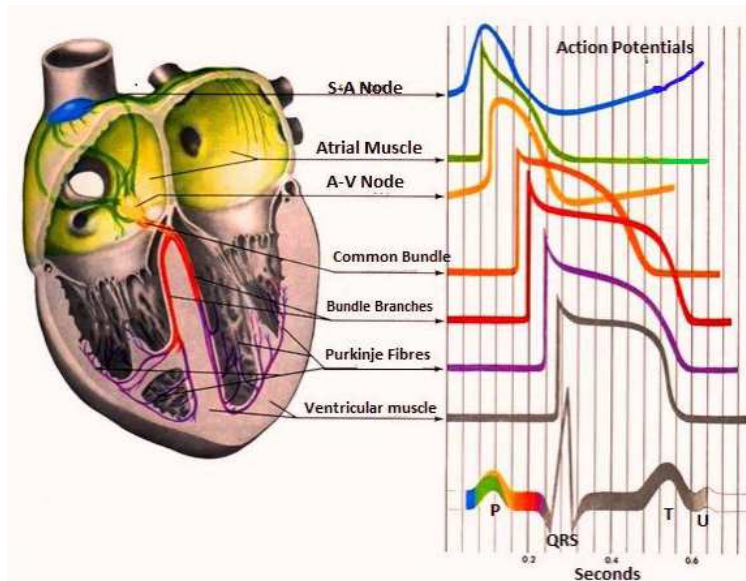


Figure 3.2: Electrical system of the heart

The electrical impulse is initiated in the sino-atrial, travels to atrio-ventricular node through the atriums and generates the contraction in atrium. Then current reaches ventricles via its bundle and flows through them causing the contractions in ventricular. At last, the current reaches to the Purkinje fibers and heart tissue's re-polarization occurs. This process seems to be a complicated task but electrical signal spreads in one second from the SA node to the entire heart in less than one second. This commotion of electrical signal is recorded and measured in the EKG.

### 3.4 Introduction to Electrocardiogram (ECG)

The ECG [8] is the electrical realization of the heart, which is very well known as a non-invasive technique, used as a diagnostic tool for cardiovascular diseases. The heart's rhythm is estimated by the counting readily identifiable waves in beats per minute (bpm). As wave-shape is changed due to cardiovascular diseases and abnormalities, therefore ECG perhaps is the most commonly recognized biomedical signal which comes out as the most commonly used signal for the patient examination.

### 3.4.1 Interpretation of ECG waveform

ECG is a crucial method for patient's monitoring. However, the diagnosis efficiency is dependent on best accurate analysis of the signal. Its analysis mainly depends upon the amplitude or duration of the various waves of ECG. Analysed parameters help doctor to diagnose any heart abnormality.

ECG is also known as heart wave, and is projection vector of the heart's electrical activities over time. ECG shows electrical activity of the heart with respect to different reference planes over a period of time. It is recording of the heart's electrical activity among one of the views. Each part of wave reflects a particular action in heart producing a unique deflection on the ECG. These deflections are recorded as a continuous group of positive and negative waves. On a normal ECG, there are mainly up to five visible distinct waveforms.

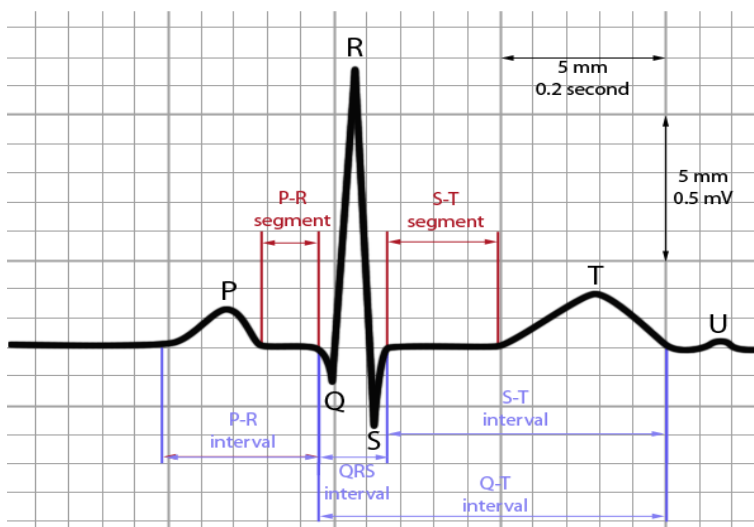


Figure 3.3: Schematic of normal sinus rhythm for a heart as seen on ECG [8]

There is a natural cardiac pacemaker that originates its own train of potentials of actions. The different sets of events and waves in sequence in cardiac cycle are as follow [13]:

1. The SA node fires.
2. Electrical activity is passed through the atrial musculature at low rates causing slow moving contraction of atria resulting in getting P-wave. Due to small size of atria and slow contraction, the P-wave is of a low amplitude.

3. The excitation wave gets a propagation delay at the atrio-ventricular (AV) node, which lead normally to iso-electric segment of about  $60 - 80ms$  after the P-wave, known as the PQ segment. The pause helps in the completion of blood transfer from the atria to the ventricles.
4. His bundle, the bundle branch and the purkinje system of specialized conduction fibers propagate the stimulus to the ventricles at the high rate. The wave of stimulus originate from the apex of the heart and move aloft, causing quick depolarization of the ventricles. This results in the QRS wave of the ECG, which is a sharp triphasic wave of about  $1mV$  amplitude and  $80ms$  duration.
5. Ventricles muscle cells have a relatively long action potential duration of about  $300 - 350ms$ . The plateau of the potential of action lead to the iso-electric segment of duration of the  $100 - 120ms$  after the QRS, known as the ST segment.
6. Re-polarization of the ventricles lead to the slow T-wave having an amplitude of  $0.1 - 0.3mV$  and duration of  $120 - 160ms$ .

ECG Parameters	Amplitude(mV) and wave duration(seconds)
P	0.25 mV
R	1.60 mV
Q	25 percent of R-wave
T	0.1 to 0.5 mV
P-R	0.12 to 0.20 seconds
Q-T	0.35 to 0.44 seconds
S-T	0.05 to 0.15 seconds
P wave interval	0.11 seconds
QRS interval	0.09 seconds

Table 3.1: Normal ECG's Amplitudes and Duration [8]

Parameters in waveform of ECG may be described as:

1. **P-wave** - It is the first deflection of the heartbeat and is the small upward wave. It denotes atrial depolarization. The initial portion of the P-wave is mainly the reflection of right atrial depolarization and the terminal portion is mainly the reflection of left atrial depolarization. All the P-waves should look alike and are not larger than  $0.3mV(3mm)$ .
2. **Q-wave** - It is immediate initial downward deflection after the P-wave. The normal Q-wave indicates septal depolarization. The Q-wave after a heart attack may be wide and deep. Hence the ECG picks up current flowing away from this muscle,

hence producing a strong negative deflection.

3. **R-wave** - The immediate upward deflection after the P-wave (and even if Q-waves are not present). The R-wave is often the easiest waveform to locate on the ECG and indicates early ventricular depolarization.
4. **S-wave** - It is the immediate negative deflection after the R-wave. It indicates the late ventricular depolarization.
5. **T-wave** - This indicates re-polarization of the ventricles. It is often upright, rounded, and little bit asymmetric. Its morphology modifies with holding of breath.

### 3.5 Processing and Analysis of ECG

Biomedical signals are mainly recorded for monitoring (detecting or estimating) specific pathological/physiological states for diagnosis and evaluating therapy. They are also used for decoding and eventual modeling of specific biological systems. Furthermore, these signals can consist of multiple channels [13]. This leads to the additional signal-processing challenges to find physiologically and meaningful interactions among these channels quantitatively.

Goals of signal processing in these cases are normally noise removal, accurate quantification of signal model and its components through proper analysis, extraction of features and predicting future functional events. Typical biological applications may involve the use of signal-processing algorithms [15] for many reasons.

The monitored biological signal is combination of signal and noise. Noise is any signal which is not synchronous and not correlated with the physiology of interest. Therefore different situations have different assumptions for noise characteristics, which will finally lead to a fitting choice of signal-processing method.

Illustration of typical steps and processes involved in diagnosis based upon signal analysis is shown in Figure 3.4

1. Signal Acquisition: Acquisition is basically divided as invasive or non-invasive and active or passive. Generally ECG being a non-invasive technique is acquired in passive way.

- Single lead- It helps in knowing wave shapes, signal spectra and conveys the repeatability of cardiac signal.
- Multiple lead- It can use additional information like concurrent features from other leads. This may provide more immunity from interfering signals.

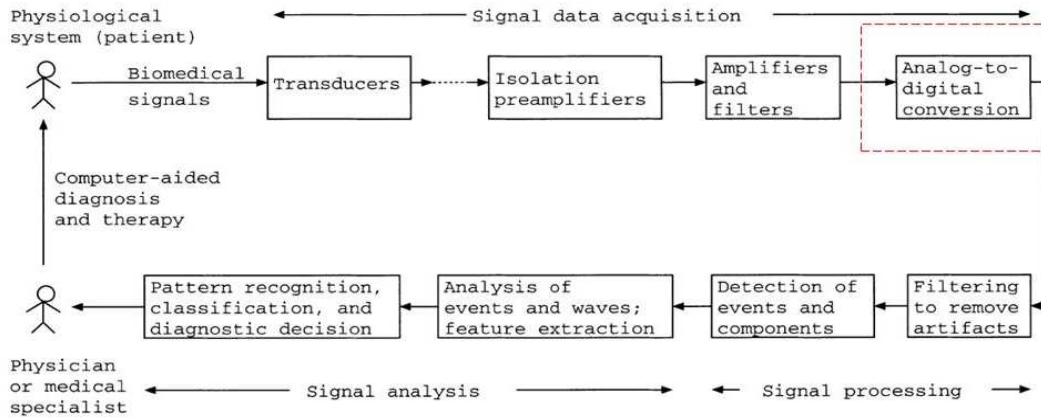


Figure 3.4: Biomedical signal processing and analysis [8]

2. Pre-processing and filtering: ECG can get corrupted by different types of noise such as wander noise, Electromyographic (EMG) interference and motion artifacts etc. The ECG signal corrupted due to these noises, leads to wrong diagnosis. Therefore, to circumvent or remove the noises, filtering [13] is widely used in biomedical signal processing.
3. Detection of events: Analysis of ECG signal for monitoring purpose needs identification of epoch (part of signal which is related to specific event of interest) and investigation of the corresponding events. Once an event is identified, the corresponding waveform is divided into parts and analyzed in terms of its amplitude, morphology, time duration, frequency content etc. Hence event detection [14] is an vital step in signal analysis.
4. Pattern Recognition: Final aim of signal analysis is the classification of given signal in one of the categories and deciding the condition of patient.

### 3.5.1 ECG Electrode Placement and ECG Leads

“Lead” refers to the voltage between two electrodes. Each lead looks at heart with different angle. Many views, each called a lead, looks for voltage changes between electrodes

placed in different position on the body. In 12 lead ECG, total 10 surface electrodes are attached to various specified positions on the body, and for impedance matching between skin and electrode suitable gel is used.

Important beneficial characteristics of the electrodes designed to pick up signals from biological objects is that they should not polarise even when small current is passed. Ag-AgCl electrodes gives  $2.5mV$  potential difference over  $10mV$  for stainless steel electrode. Proper coating of silver chloride is applied to a silver electrode which minimizes the electrical impedance and hence sensitivity is increased. The 10 electrodes are classified as:4 limb electrodes; Right Arm (RA), Left Arm (LA), Left Leg (LL) and Right Leg (RL), 6 chest electrodes; V1-V6. Total 12 Leads are derived from these 10 electrodes. These 12 leads are further classified as 3 limb leads, 3 augmented limb leads and 6 precordial leads. Out of these 12 leads, limb leads are bipolar while all other leads are unipolar leads. The definition for all 12 leads [8] is as follows,

1. Lead I, signal between negative RA and positive LA electrodes
2. Lead II, signal between negative RA and positive LL electrodes
3. Lead III, signal between negative LA and positive LL electrodes.

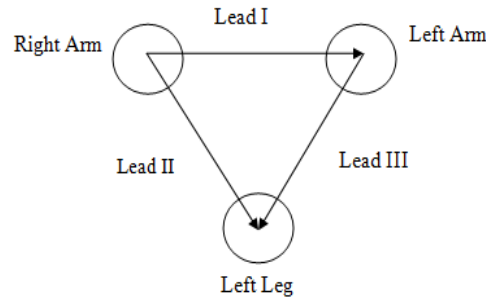


Figure 3.5: Einthoven's triangle

These three limb leads form the points of Einthoven's triangle as shown in Figure 3.5, which is the theoretical triangle drawn around the heart with heart at centre. According to Einthoven's law,

$$\text{Lead I} - \text{Lead II} + \text{Lead III} = 0$$

4. Lead aVR or vector right Augmented – Signal between positive electrode on RA and the negative electrode, which is the combination of LL and LA.

5. Lead aVL or vector left Augmented – Signal between the LA on positive and the combination of RA and LL on negative electrode.
6. Lead aVF or vector foot Augmented Signal between LL and combination of RA and LA with positive and negative sign respectively.
7. Precordial leads V1-V6 Signal between the positive V1-V6 electrode on the chest and the electrode, which is negative of the Wilson terminal obtained by adding three limb leads.

### 3.6 Noises in ECG

Electrocardiogram (ECG) signal is an electrical recording of activity of heart. It is in the range of small voltage of magnitude  $10V$  for fetal and  $5mV$  for adult, and has a component of frequency from about  $0.05 - 100Hz$ . The ECG often gets interfered with various noises, which can be around the interested band of frequencies and identical in nature to the morphology of the ECG itself. Various noises are described below [15] :

1. EMG related to coughing, breathing, or squirming affecting the ECG - EMG is because of muscle's contractions and burst duration. It normally lasts around 50ms between dc and 10,000 Hz with 10% amplitude level.
2. Heart sound is affected by bowel movement, breath and lungs i.e., phonocardiogram (PCG).
3. Muscle sound called as vibromyogram (VMG) and interference in sound joint i.e., vibroarthrogram (VAG).
4. Maternal ECG getting mixed with the fetal ECG.
5. Electrical interference external in nature to the subject and recording system.
6. High-frequency noise in the ECG.
7. Artifacts of motion in the ECG - These are because of either the movement of patient or loss of electrode contact and baseline changes caused by modification in electrode motion.

8. Noise due of electrode skin contact impedance variations.
9. Power - line Interference in ECG signals - Data cables which carry ECG signal from the patients to displays are affected by Electromagnetic interference (EMI) coming from the 50/60 Hz power line noise. This noise make the quality of signal a bit inferior and affects the minute features which can be crucial for diagnosis.
10. Baseline Drift can be viewed as a sinusoidal component in nature at the frequency of respiration added to the ECG signal. It is usually of respiratory nature with amplitude of around 5% at frequencies between 0.15 and 0.3Hz. The drift creates problems in ECG signal detection, e.g., amplitude of T-wave gets higher than the R-wave peak which lead to untrue detection of R-peak.
11. Noise generated by electronic devices used in signal processing circuits. There are other types of noises which contaminates ECG signal like instrumentation noise, electrosurgical noise and other less significant source of noise.

### 3.7 Artifacts Removal

An ECG signal should be as clean and clear as possible so that physicians and doctors are able to make decisions accurately. As an electrical signal, ECG is prone to different kinds of noise so, filtering is necessary to remove noise without degrading the signal quality. Various noises that corrupt ECG are presented in Section 3.6. Out of them some noises can be filtered using time domain processing techniques whereas others can be filtered out using frequency domain techniques. So based upon filtering in time or in frequency domain, we can classify the filters in categories:

1. Time-Domain Filters- Time-domain filters or digital filters do not require prior knowledge of signal and noise spectral characteristics.
  - Synchronised averaging: These are used when noise is overlapped with signal. This removes repeated signal and noise from the main signal. Also it improves the signal SNR. Power line interference, background EEG from ERPs and SEPs can be made to suppress using this method.
  - Moving-average filters: It eliminates high frequency noises.
  - Derivative-based filtering: These are used where DC component and low fre-

quency component are to be suppressed. Base-line drift is removed by this method.

2. Frequency-Domain Filters- These are used when specific high pass, low pass, band-pass and bandstop characteristic is intended.

- Butterworth low pass filter: Used to remove high frequency component in specific band.
- Butterworth high pass filter: It removes low frequency noises.
- Notch and comb filters: These are used when periodic artifacts are to be removed. Power-line interference is also removed by this filter.

Apart from time and frequency domain filtering approaches, we also have Optimal Filtering and Adaptive filtering techniques. They are helpful when interference is non-stationary.

### 3.8 Abnormalities in ECG

The normal rate of heart is 60 to 100 beats per minute. A rate slower than the normal range is called bradycardia (slow heart) and a rate higher is called tachycardia (fast heart). Arrhythmia is indicated by ECG not being normal. Heart rate is simply count

ABNORMALITY	CHARACTERISTICS
Bradycardia	R-R interval $\geq 1s$
Tachycardia	R-R interval $\geq 0.6s$
Hypercalcaemia	QRS interval $\geq 0.1s$
Dextrocardia	Inverted P-wave
Hyperkalemia	Tall T-wave and absence of P-wave
Sudden cardiac death	Irregular ECG
Sinoatrial block	cardiac cycle complete drop out
Myocardial ischemia	Inverted T-wave

Table 3.2: Abnormality in ECG [13]

of heart beats per minute (bpm). Average heart rate of human is 72 times in a minute. Heart rate is low during sleep and is 70 bpm while during activity it is 60 bpm. The abnormalities are shown in Table 3.2. When heart rate is below 60bpm, disorder is termed as bradycardia and when it is high it is termed as tachycardia.

## 3.9 S-transform

The advantages of STFT are combined with WT to get ST. In ST, analysing window's height and width are scaled with changes in the frequencies. Also, ST simultaneously localises the real and imaginary spectra along with having a resolution [9] depending on frequency. This makes information of frequencies more obvious than in WT and STFT.

### 3.9.1 Deduction from STFT and wavelet

**1. Deduction from STFT** FT lacked on the part of localization of time frequency. Gabor's idea of introducing a Gaussian window capable of scalable moving as in (1.2). The Gaussian window succeed to combine domains of time and frequency with uncertainty of the lower bound whose equation given in (??). The Gaussian window is defined as

$$\omega(t) = \frac{1}{\delta\sqrt{2\mu}} e^{-\frac{t^2}{\delta^2}} \quad (3.1)$$

here,  $\delta$  is a factor of scale and to make it more adaptable [11],  $\delta$  is defined as  $\delta(f) = \frac{1}{|f|}$ , to make it function related to frequency. And also this window should be 1 mean, as follows:

$$\int_{-\infty}^{+\infty} \omega(t, f) dt = 1 \quad (3.2)$$

Therefore the expression we got for ST as:

$$ST(t, f) = \int_{-\infty}^{+\infty} x(t) \omega(t - \tau, f) e^{-j2\pi ft} dt = \int_{-\infty}^{+\infty} x(t) \frac{|f|}{\sqrt{2\pi}} e^{-j2\pi ft} dt \quad (3.3)$$

Thus localizing Gaussian window in inverse frequency domain is an improvement over the window having fixed width used in the STFT [2].

### 2. Deduction from Wavelet

The definition of continuous wavelet transform (CWT) is

$$W_c(\tau, d) = \int_{-\infty}^{+\infty} x(t) \omega(t - \tau, d) dt \quad (3.4)$$

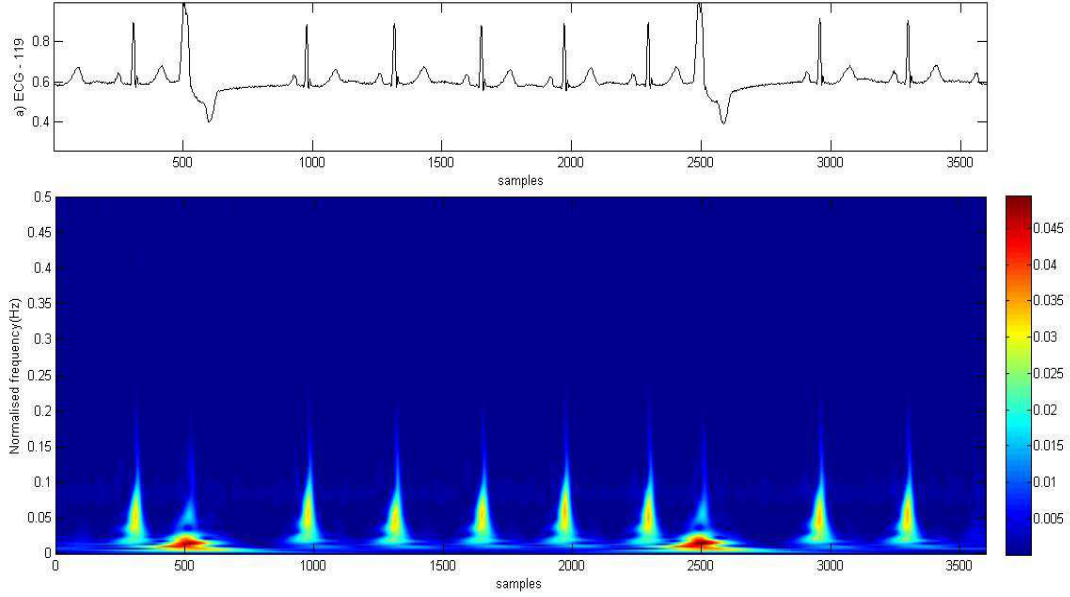


Figure 3.6: ECG signal and ST spectrum

Mother function of wavelet  $\omega(t, d)$  is to be agreed on the admissibility condition of mother wavelet [6]. So the mother wavelet is defined as:

$$\omega(t, f) = \frac{|f|}{\sqrt{2\pi}} e^{-j2\pi ft} \quad (3.5)$$

The ST is termed as a continuous wavelet function with a special mother wavelet multiplied by the factor of phase

$$S(t, f) = e^{j2\pi ft} \int_{-\infty}^{+\infty} x(t) \omega(t - \tau, f) dt \quad (3.6)$$

Also the dilation factor  $d$  is the inverse of frequency  $f$  and the admissibility condition is not satisfied by the wavelet function given by 3.4. Hence we get the ST given by 3.3

### 3.9.2 Inverse S-transform

ST is a representation of local spectrum. Fourier spectrum can be found by simple mean over the local spectra.

$$X(f) = \int_{-\infty}^{+\infty} S(\tau, f) d\tau \quad (3.7)$$

Relationship between Fourier and S-transform as given by:

$$X(f) = \int_{-\infty}^{+\infty} x(t) e^{-j2\pi ft} dt = \int_{-\infty}^{+\infty} S(\tau, f) d\tau \quad (3.8)$$

S-Transform can be used to recover the signal exactly as:

$$x(t) = \int_{-\infty}^{+\infty} \left\{ \int_{-\infty}^{+\infty} S(\tau, f) d\tau \right\} e^{j2\pi ft} df \quad (3.9)$$

### 3.9.3 Discrete S-transform

The discrete version of ST takes advantage of computational efficiency of fast Fourier transform (FFT) and the convolution theorem. The implementation procedure of discrete S-transform is shown. The calculation procedure of discrete S-transform is as follows:

1. Calculation of Discrete Fourier Transform (DFT) of signal  $x(k)$  with a sampling time interval of  $m$ , we will have  $H(m)$  and making a frequency shifting  $n$ , we get  $H(m+n)$ .

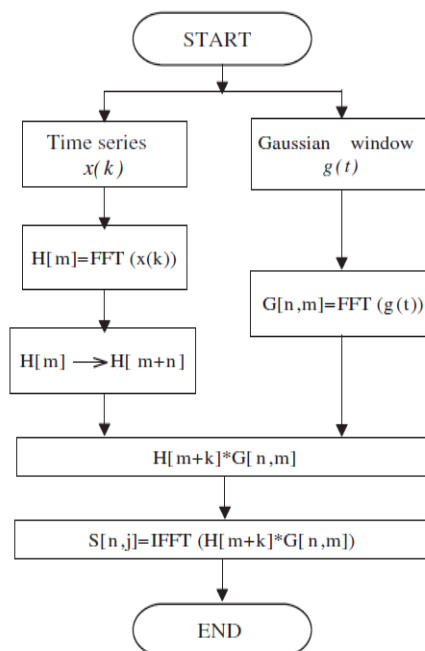


Figure 3.7: Implementation of Discrete ST

2. Calculate DFT of gaussian window  $g(t)$  at a specific  $n$ , which is called a voice

Gaussian. The voice Gaussian is given by  $G(n, m)$ .

3. Multiply  $G(n, m)$  by  $H(m + n)$  to get  $B(n, m)$ . ST can be restored by fast fourier inverse transform.

So, overall ST is an invertible transform which merged the merits of WT and STFT. Providing progressive resolution and multi-scale resolution makes ST very useful in various practical applications. It has been used in the field of biomedical research such as identification of genetic abnormalities in brain tumours, in examination of psychiatric disorders, sclerosis lesion's early detection and ECG and audio recordings analysis for checking cardiac abnormalities. ST has also been applied on non-biomedical tasks like investigation of disturbances in electrical power distribution networks and detection of gravitational waves. ST and FrFT [10] are combined together to form a new tool called as fractional S-transform given by Xu De-Ping in 2012 for analysis of fractional frequency domain.

## 3.10 Fractional ST- A novel JTFA Tool

FrST being the joint time-frequency tool [11] enhances the resolution of time and frequency concurrently. With the change in parameters of FrFT, fractional-frequency axis gets rotated and more information may be obtained from the signal. Therefore it enhances the flexibility of processing signal spectrum.

### 3.10.1 Theoretical and Mathematical Background

FrST is the extension of ST of time frequency domain to domain of time fractional frequency. So basically we can consider FrST as, ST defined in fractional domain. Also FrST can be considered as localised FrFT as it takes one dimension function to two dimension resulting in instantaneous fractional fourier frequency spectrum. On multiplying fractional Gaussian window and the signal and then taking FrFT, FrST is obtained as in (3.10) which was also mentioned in Section 1.6.

$$FrST_x^a(\tau, u) = \int_{-\infty}^{+\infty} x(t) g(\tau - t, u) K_a(t, u) dt \quad (3.10)$$

where  $K_a(t, u)$  is the FrFT kernel and  $g(\tau - t, u)$  is a scalable Gaussian window function depending on time  $t$  and  $u$  is the fractional fourier frequency. Kernel and Gaussian

window are defined as:

$$K_\alpha(t, u) = \left\{ \begin{array}{l} \sqrt{1 - j \cot \alpha} \exp [j\pi (u^2 \cot \alpha - 2ut \csc \alpha + t^2 \cot \alpha)], \alpha \neq n\pi \\ \delta(t - u), \alpha = 2n\pi \\ \delta(t + u), \alpha = (2n \pm 1) \pi \end{array} \right\} \quad (3.11)$$

where  $p, q$  are the factors of adjustment for window,  $\alpha$  is a fractional parameter given by:

$$\alpha = \frac{a\pi}{2} \quad (3.12)$$

One of the parameters of FrST is  $\alpha$  which relies on factor of rotation rotation factor  $a \in [0, 4]$ , also called as the order of FrST. Depending upon the value of  $a$ , fractional frequency axis  $u$ -axis is rotated. Gaussian Window shape is changed depending upon  $p, q$  and its width is altered by  $u$ . Therefore we can conclude that FrST depends on 3 factors and thus it is fractional fourier approach which is adaptive in time.

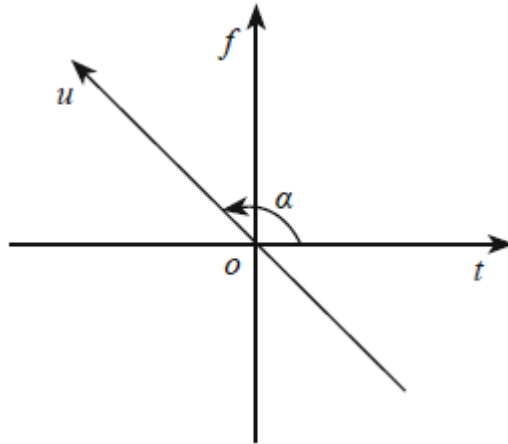


Figure 3.8: Time and fractional fourier frequency domain plane

Figure 3.8 shows the fractional fourier frequency domain, which is nothing but the rotated version of  $t$ - $f$  plane. Rotation depends on the rotation parameter  $a$  by the relation described in (3.12).  $t$ - $f$  gets transformed to fractional fourier frequency domain by this relation.

### 3.10.2 Deduction of FrST from ST and FrFT

The  $a^{th}$  order FrFT of a signal is defined as [12]:

$$x_a(u) = F^a[x(t)] = \int_{-\infty}^{+\infty} K_a(u, t) x(t) dt \quad (3.13)$$

where  $x(t)$  is the signal,  $K_a(u, t)$  is the FrFT kernel and  $a$  is the order and  $x_a(u)$  is the fractional Fourier transform of  $x(t)$ . FrFT can be thought of as time and frequency rotation. Applying the rotation property of TFD we get the relation between FrFT and ST which is nothing but the FrST [12]:

$$FrST_x(t, f) = R_\phi \{ST_{x_a}(t, f)\} \quad (3.14)$$

where  $R_\phi$  is the rotation operator which defined as:

$$R_\phi = \begin{pmatrix} \cos\phi & \sin\phi \\ -\sin\phi & \cos\phi \end{pmatrix} \quad (3.15)$$

Using relation one can shift from fractional frequency domain to time frequency. Also, by employing the properties written below of shifting in time and shifting in frequency of FrFT on (3.14)

$$F^a[x(t - \tau)] = e^{j\pi\tau^2 \sin\phi} x_a(u - \tau \cos\phi) e^{-j2\pi u \tau \sin\phi} \quad (3.16)$$

$$F^a[e^{j2\pi\tau f} x(t)] = e^{-j\pi f^2 \sin\phi \cos\phi} x_a(u - f \sin\phi) e^{j2\pi u f \cos\phi} \quad (3.17)$$

Using these properties in eq3.14, we get

$$\begin{aligned} |FRST_x(t, f)| &= \left| R_\phi \left\{ \int_{-\infty}^{+\infty} x_a(\tau) \cdot g(\tau - t, f) \cdot e^{-j2\pi f \tau} d\tau \right\} \right| \quad (3.18) \\ &= \left| R_\phi \left\{ \int_{-\infty}^{+\infty} \int_{-\infty}^{+\infty} x(t') K_a(t', \tau) x(t') dt' \cdot g(\tau - t, f) \cdot e^{-j2\pi f \tau} d\tau \right\} \right| \\ &= \left| R_\phi \left\{ \int_{-\infty}^{+\infty} x(t') \left[ \int_{-\infty}^{+\infty} g(\tau - t, f) \cdot e^{j2\pi f \tau} \cdot K_{-a}(t', \tau) d\tau \right]^* dt' \right\} \right| \\ &= \left| R_\phi \left\{ \int x(t') \cdot \{FRFT_{-a}[g(\tau - t, f) \cdot e^{j2\pi f \tau}]\}^* dt' \right\} \right| \\ &= \left| R_\phi \left\{ \int x(t') \cdot e^{j\pi(t^2 - f^2) \sin\phi \cos\phi} g_{-a}^*(t' - t \cos\phi + f \sin\phi, f) e^{-j2\pi t'(t \sin\phi + f \cos\phi)} dt' \right\} \right| \end{aligned}$$

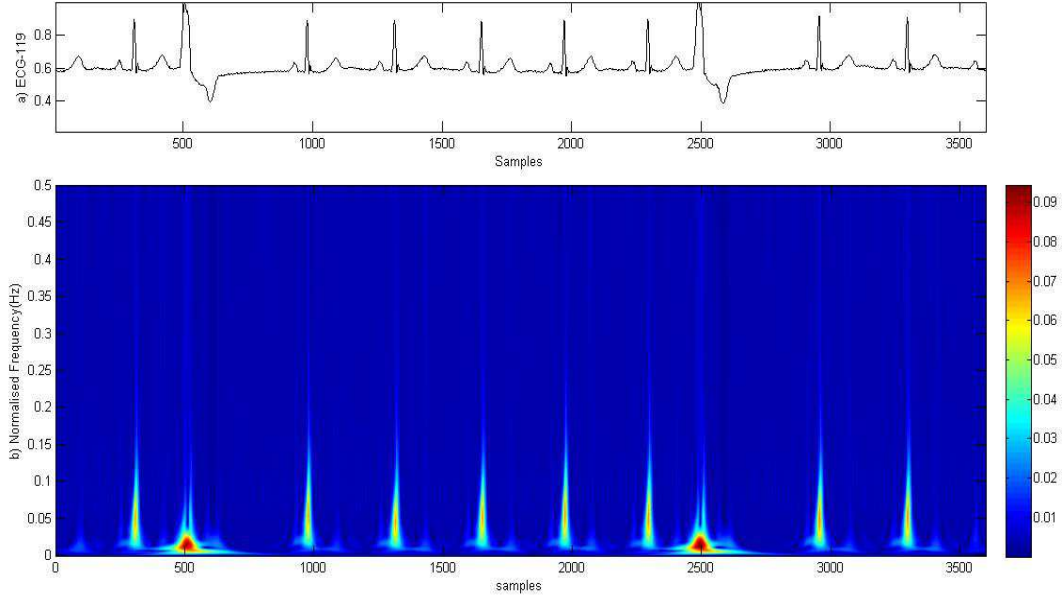


Figure 3.9: ECG signal and FrST spectrum

$$\begin{aligned}
 &= |R_\phi \{ R_{-\phi}^{-1} \int x(t') [g_{-a}^*(t' - t, f) e^{-j2\pi t' f}] dt' \}| \\
 &= |\int x(t') . g_a(t' - t, f) e^{-j2\pi t' f} dt'|
 \end{aligned}$$

FrFT of the Gaussian window is also a different shaped Gaussian window. Thus, the timefrequency plane will not be changed by the Gaussian window which is fractional. Thus, the actual plane of FrST retains the the time-frequency plane . And the local spectra representation with high resolution can be obtained by adding the Gaussian window to the signal which is fractional.

### 3.11 Uncertainty principle and FrST

The criterion for evaluation of time-frequency aggregation can be time-bandwidth product (TBP). Durak and Arikan proposed the concept of generalised time-bandwidth product (GTBP), that is the lengthening of TBP in fractional domain, defined as

$$GTBP \{x(t)\} = \min_{0 \leq a \leq 4} TBP \{x_a(t)\} \quad (3.19)$$

where  $x_a(t)$ , 'a' order of FrFT of signal  $x(t)$ . we have to minimize TBP for particular value of rotation factor  $a$  to find the optimal order of time-frequency analysis in the domain

which is fractional.

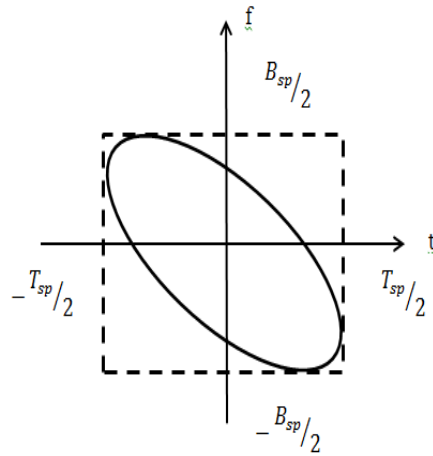


Figure 3.10: Compact support set of signal in time-frequency plane

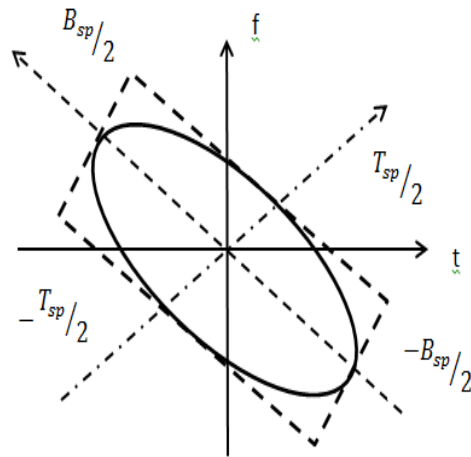


Figure 3.11: Compact support set for signal with optimal order

In time-frequency analysis, addition of window to signal changes the time width of signal to windowed signal's time width and bandwidth becomes windowed signal's bandwidth. Relation between this transformation is given by:

$$T_{sp} = T_s \sqrt{1 + \left(\frac{T_h}{T_s}\right)^2} \quad (3.20)$$

$$B_{sp} = B_s \sqrt{1 + \left( \sqrt{\frac{B_h}{B_s}} \right)^2} \quad (3.21)$$

where  $T_s$  and  $B_s$  are original signal's time width and bandwidth,  $T_h$  and  $B_h$  are window's time width and bandwidth, and  $T_{sp}$  and  $B_{sp}$  are windowed signal's time width and bandwidth.

# Chapter 4

## JOINT TIME-FREQUENCY ANALYSIS OF ECG

Electrocardiography [8] is the most popular tool for diagnosing and detecting heart disorders. During ECG acquisition, signal gets interfered by different noises, due to which our signal gets contaminated. Therefore it is necessary to remove unwanted noise that degrades the quality of ECG signal. Noise sources that corrupt ECG can either be cardiac or extra-cardiac. Prolonged re-polarization, atrial flutter, reduction or disappearance of the isoelectric interval are some examples of cardiac noises and extra-cardiac noises like muscle contraction, power line interference, respiration can occur. All these noises make the analysis difficult and error prone, hence noisy ECG should be denoised by removing noise components for analysing it further. This will make easy for physicians to accurately evaluate cardiovascular diseases.

A good denoising approach is capable of removing noises by filtering the signal and by ensuring a result as close as possible to actual signal. Numerous researchers have reported various techniques for denoising ECG signals in literature such as wavelet denoising, adaptive filtering, empirical mode decomposition and wiener filtering. These methods generally involve the removal of unwanted artifacts present in the known and limited spectrum range of ECGs. Approaches presented in this chapter is based on the analysis of signal in time-frequency domain. These methods helps to represent signal in time frequency domain and hence are suitable for performing operations such as masking and thresholding for getting the clean ECG signal. Various performance metrics are used to prove the results better than the existing methods [15].

### 4.1 ECG denoising using ST

ST provides great flexibility and utility for processing non-stationary signal due to its progressive resolution. ST has much better performance in noisy environment than that

of conventional methods, such as wavelet denoising, adaptive filtering etc. ST uniquely combines absolute phase information with frequency dependent resolution. Also, as it is based on the superior time-frequency resolution, the ST spectrum can be described effectively [31].

### 4.1.1 Methodology

The objective of the algorithm is to denoise signal by selecting the frequency in range of interest and decreasing the noise counterpart. The approach is described in Figure 4.1. Different steps involved in the algorithm are explained below:

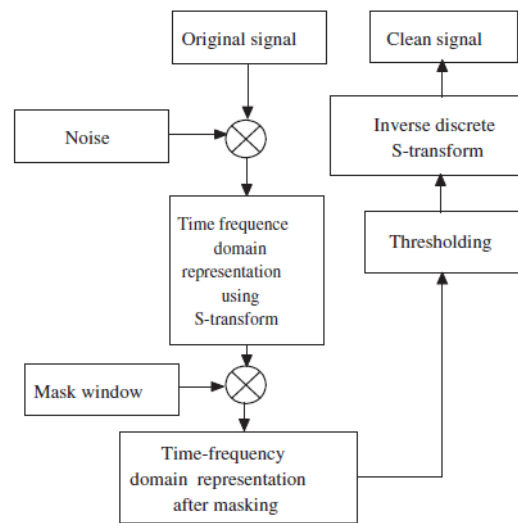


Figure 4.1: Block diagram for ECG denoising method ST

**Step 1 :** Collection of Database: MIT/BIH arrhythmia database (MITDB)[20] is selected for ECG signal analysis. This database has 48 ECG signals of half hour duration, sampled at  $360Hz$  in accordance with Nyquist's Rule at 11 bit resolution. 11 tapes of ECG data records are selected out of which 5 are normal and rest are abnormal records. The random noise generated in MATLAB is added to the records to validate the process of denoising.  $h(t)$  and  $n(t)$  are the representation of original and noisy ECG signals that will be used further.

**Step 2 :** Time-frequency( $t - f$ )domain representation: Apply ST on the original signal and noisy ECG signal. The flowchart of discrete ST is shown in Figure 4.2.

1. FFT of the N-point time series is calculated.

2. FFT spectrum is shifted to make voice frequency zero.

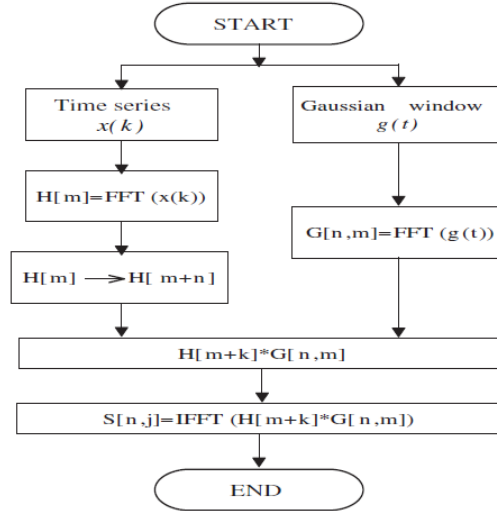


Figure 4.2: Flowchart for calculating Discrete ST [31]

3. N-point Gaussian window is multiplied with output of step 2.

4. N-point IFFT is calculated to obtain the corresponding frequency.

5. These steps are iterated for all the voice frequencies.

**Step 3 : Masking:** Clean ECG has bandwidth of  $0.05 - 100Hz$ . The data available in MITDB contains important information within  $200Hz$ . Hence mask window is chosen such that it is unity in required range of frequencies and zero everywhere else. Masking is done by multiplying the mask window with output of previous step i.e., with noisy ECG in time-frequency domain.

**Step 4 : Thresholding and filtering:** This step removes the background noises which are present between the QRS complex in time-frequency domain. Adaptive threshold technique is used to eliminate background noises. In filtering, we apply smoothing operation on the boundaries of masked output.

**Step 5 :** As ST is exactly invertible, the denoised ECG in time domain is obtained after performing inverse ST on the matrix, achieved after masking and thresholding [29].

Figure 4.3 shows  $t-f$  domain representation of record no.119, taken from MITDB. The color bar shows the relation between amplitude spectrum and color. Masking is done to remove high frequencies and is shown in Figure 4.4. Thresholding and filtering is done to remove the residual noise after masking. Figure 4.5 represents the final output in

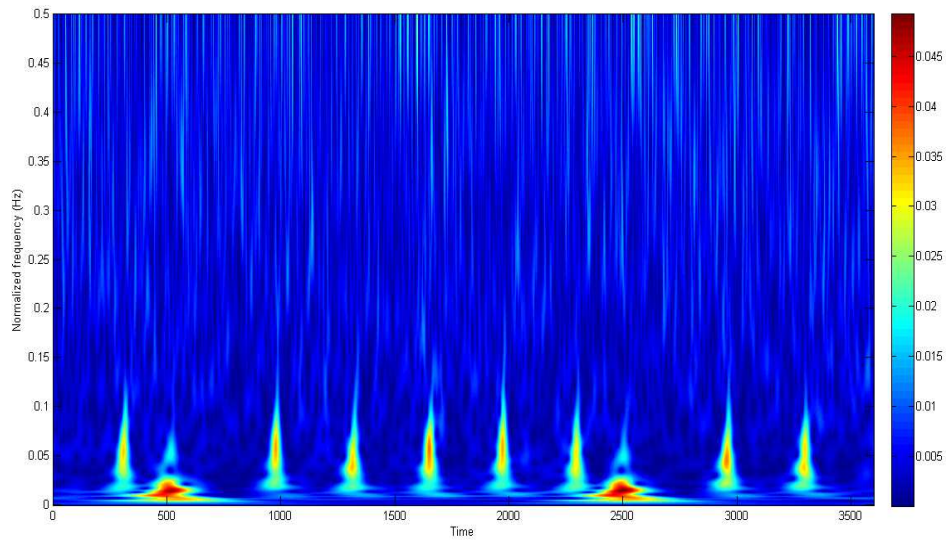


Figure 4.3: ST of a noisy ECG record 119

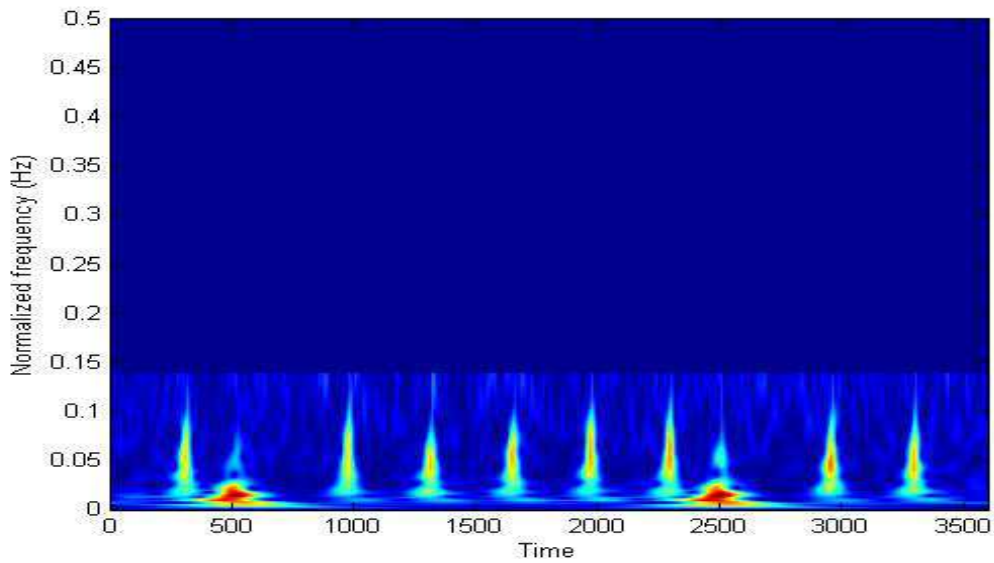


Figure 4.4: T-f distribution of noisy ECG record 119 after masking

$t$ - $f$  domain, on which finally inverse ST is applied to get signal back in time domain. Denoised signal is shown in Figure 4.6.

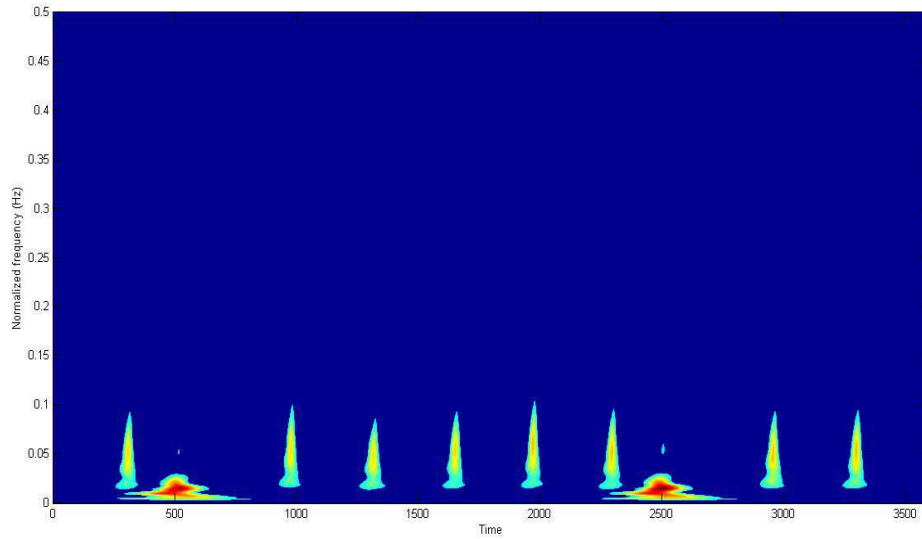


Figure 4.5: T-f distribution obtained after thresholding and filtering

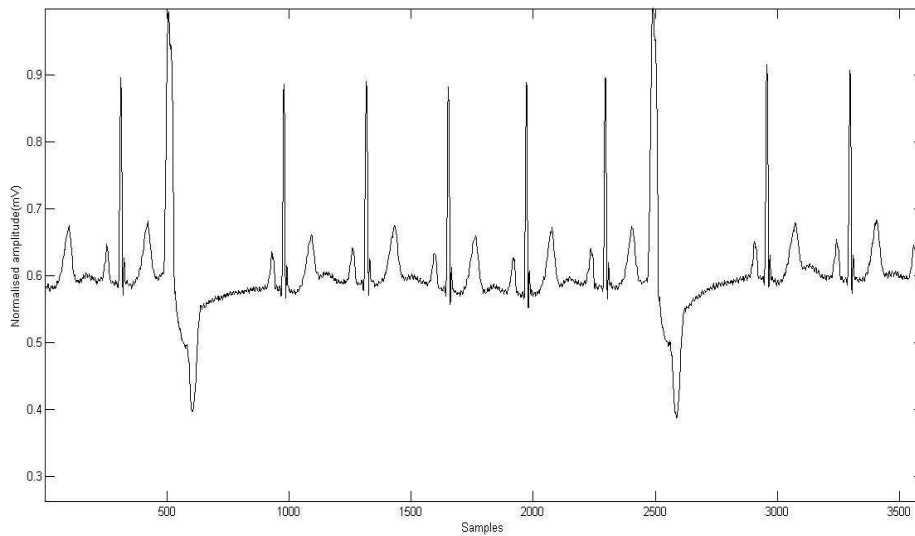


Figure 4.6: Denoised ECG signal

## 4.2 Denoising using FrST

FrST is the latest time fractional frequency tool that has only been applied in area of geophysics so far. FrST has better time-frequency concentration. As mentioned in Section 3.10, FrST is the combination of FrFT and ST. It is also observed that with the adjustment of FrST parameters at  $a = 1, p = q = 1$ , we get  $\alpha = \frac{\pi}{2}$ , FrST is reduced to ST, so FrST has all the advantages of ST [2,11].

## 4.2.1 Proposed Methodology

The proposed methodology is described in Figure 4.7 and different steps involved are described as:

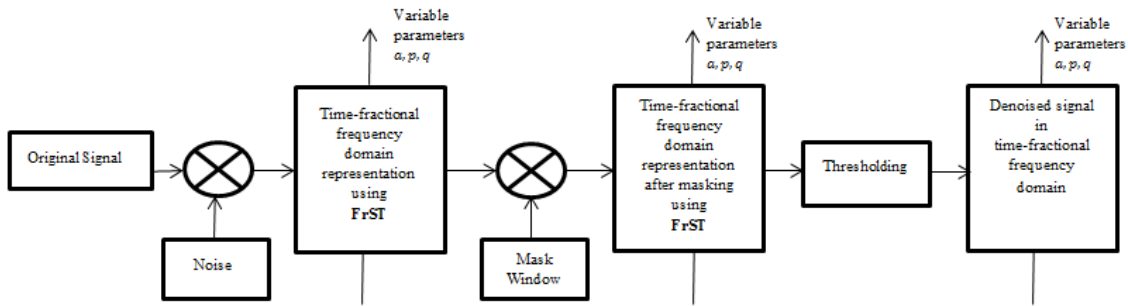


Figure 4.7: Block diagram for proposed ECG denoising method

1. Time fractional frequency domain representation - FrST is applied on the signals chosen in Section 4.1.1. MATLAB generated random noise is added to the signals for validating proposed algorithm. Figure 4.8 shows the signal in time fractional fourier domain.

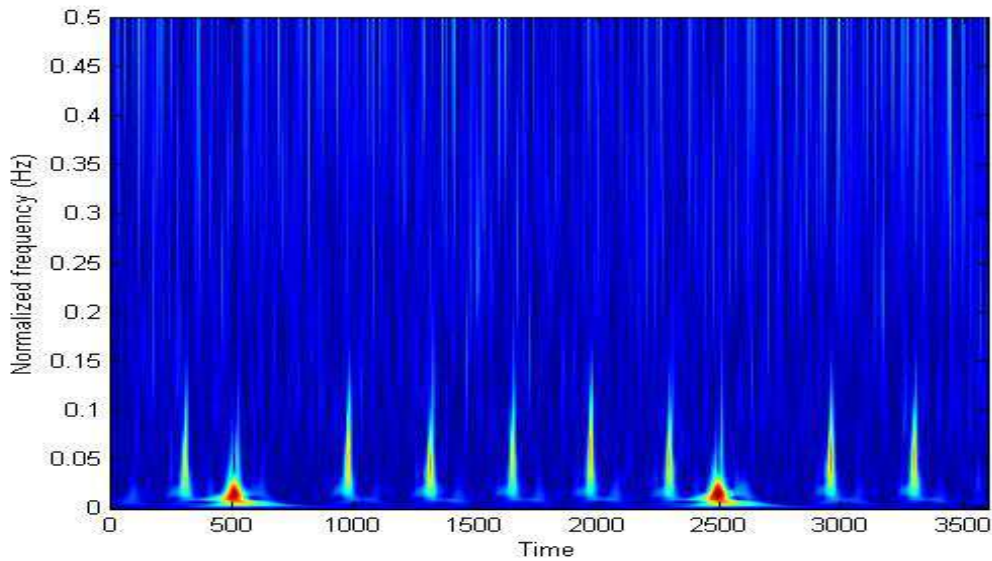


Figure 4.8: Time-fractional frequency domain representation of ECG signal record 119

2. Masking - It is done to remove high frequencies. Mask window is a unity mask window having value unity at desired frequencies. Figure 4.9 shows the output after masking is performed.

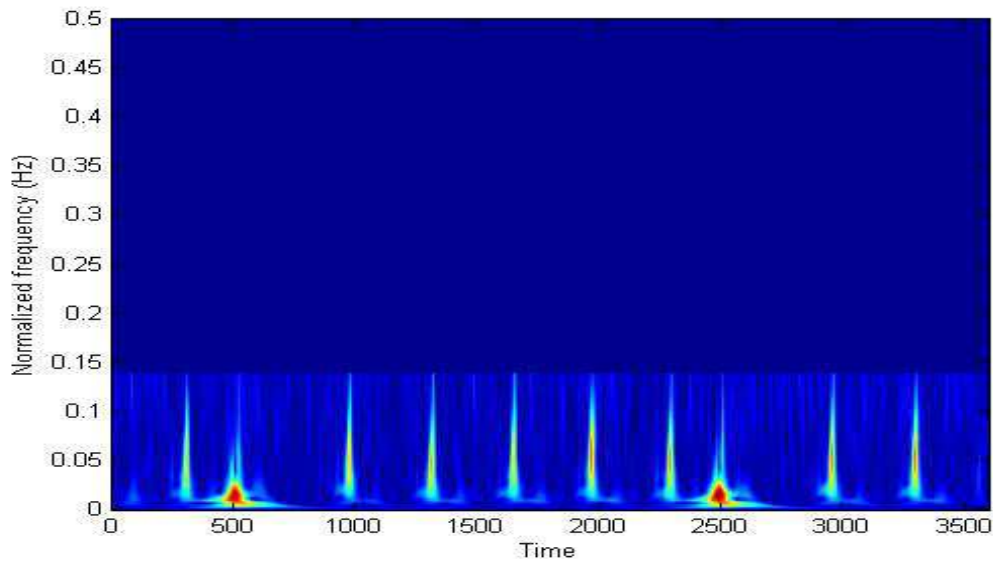


Figure 4.9: Time-fractional frequency domain representation after masking

3. Thresholding - This is done to eliminate noises present at low frequency. Adaptive thresholding is done to remove intermediate noise that shows up between the QRS complex. Figure 4.10 shows the final output in time and fractional fourier frequency domain.

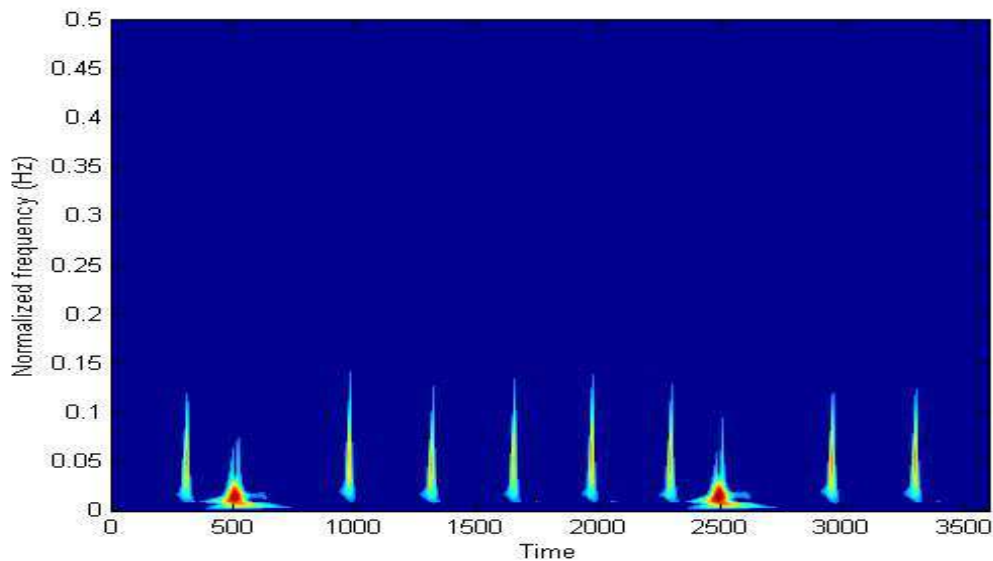


Figure 4.10: Time-fractional frequency domain representation after thresholding

Algorithm described in this section and previous section is almost same but the differences arises in calculation of FrST and ST. Later algorithm is a adaptive algorithm,

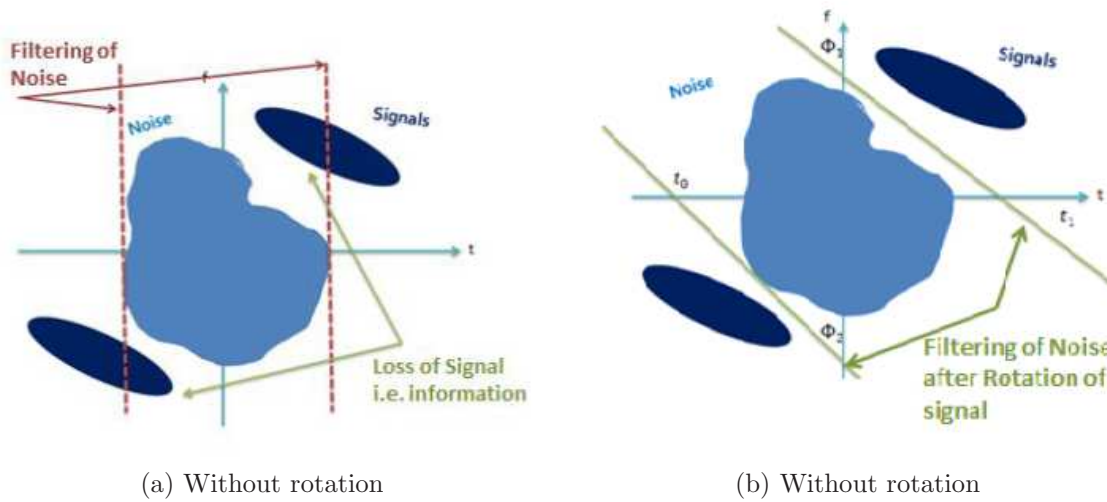


Figure 4.11: Filtering done without rotation and with rotation of signal

that is we can vary the FrST parameters  $a, p, q$  and get different outputs. This is based on the concept that as noise with constant power spectral density is not concentrated to any domain. Therefore filtering of noise should be done in the domain where the signal is highly concentrated so that noise can be easily separated out from the ECG signal.

### 4.3 Performance Metric

For evaluating the performance of the denoising methods following parameters are chosen [26]:

1. Signal to Noise Ratio(SNR),given by

$$SNR = \frac{\sum_{t=0}^{L-1} h(t)^2}{\sum_{t=0}^{L-1} n(t)^2} \quad (4.1)$$

2. Root Mean Square Error(RMSE),given by

$$RMSE = \sqrt{\frac{\sum_{t=0}^{L-1} (h(t) - \hat{h}(t))^2}{L}} \quad (4.2)$$

3. Percentage Root Difference (PRD), given by

$$PRD = \sqrt{\frac{\sum_{t=0}^{L-1} (h(t) - \hat{h}(t))^2}{L}} * 100 \quad (4.3)$$

where  $h(t)$  is the original ECG signal,  $\hat{h}(t)$  is the denoised signal,  $n(t)$  is the noise signal.

## 4.4 Results and Discussions

Quantitative analysis for denoising using ST and FrST is performed for the ECG tapes. Data used for the analysis is both with and without added noise. Noise that is added is randomly generated from MATLAB. “RMSE”, “SNR” and “PRD” is calculated. For the proposed method i.e., FrST based method, simulation is done for different values of parameter  $a$  keeping  $p$ ,  $q$  same. Values of  $p$  and  $q$  are found to give best results at  $p = 0.511$  and  $q = 0.51$ .

Record	RMSE	PRD	SNR
100	0.002	0.2045	53.7846
101	0.0016	0.1595	55.945
102	0.0023	0.2291	52.8
103	0.0017	0.1688	55.4506
113	0.0021	0.2125	53.4511
119	0.0027	0.2715	51.3254
201	0.0018	0.1779	54.9948
207	<b>0.0013</b>	0.1257	58.0157
214	0.0024	0.2425	52.307
217	0.0015	0.1467	56.6729
231	0.0018	0.1836	54.7226

Table 4.1: Performance results for ST based Denoising without added noise

Record	RMSE	PRD	SNR
100	0.0191	1.9057	34.399
101	0.0179	1.7879	34.9532
102	0.0167	1.6736	35.5269
103	0.0169	1.6863	35.4615
113	0.0159	1.5911	35.9662
119	<b>0.0145</b>	1.453	36.7548
201	0.0193	1.9296	34.2905
207	0.0196	1.9567	34.1694
214	0.0167	1.6666	35.5634
217	0.0177	1.7696	35.0426
231	0.0174	1.7392	35.1932

Table 4.2: Performance results for ST based Denoising with added noise

Record	RMSE	PRD	SNR
100	0.0016	0.1612	55.8535
101	0.0016	0.1555	56.167
102	0.0029	0.2912	50.7166
103	0.0015	0.1521	56.3546
113	0.0021	0.2092	53.5895
119	0.0024	0.2398	52.4023
201	0.0014	0.1412	57.0009
207	0.0014	0.1413	56.996
214	0.0021	0.2078	53.6483
217	0.0015	0.1543	56.2324
231	0.0019	0.1869	54.5678

Table 4.3: FrST based denoising without added noise  
with  $a=0.4$ ,  $p=0.511$ ,  $q=0.51$

Different tables are generated for 11 records. Original signal and modified signal i.e., signal corrupted by adding random noise are tested against the mentioned algorithms. Following observations are made.

- It is observed that upon adding noise, RMSE value increases and SNR decreases. It can be seen from Table 4.1 and Table 4.2 that for record 207, value of SNR is changed from 54.99 to 34.29 dB.
- For the every record, proposed method gave different values of SNR and RMSE depending upon parameters chosen. For record 207 without noise, SNR is 59.02 dB for  $a = 0.3$ , SNR is 56.99 dB for  $a = 0.4$ , SNR is 46.98 dB for  $a = 0.5$  and SNR is 36.71 dB for  $a = 0.6$ . Also, with increase in value of rotation factor  $a$ , SNR decreases and on observing the values of RMSE, it increases by increasing  $a$ .

Record	RMSE	PRD	SNR
100	0.0068	0.6801	43.348
101	0.0068	0.6823	43.3201
102	0.0072	0.7249	42.7939
103	0.0068	0.6792	43.3602
113	0.0072	0.7216	42.8346
119	0.0071	0.7133	42.9348
201	0.007	0.6971	43.1344
207	0.0069	0.6859	43.2747
214	0.0073	0.7315	42.7154
217	0.007	0.6967	43.1397
231	0.0069	0.689	43.2356

Table 4.4: FrST based denoising with added noise with  $a=0.4$ ,  $p=0.511$ ,  $q=0.51$

Record	RMSE	PRD	SNR
100	0.0046	0.4602	46.741
101	0.0042	0.4225	47.4837
102	0.0051	0.5096	45.8548
103	0.004	0.4007	47.9441
113	0.004	0.4016	47.9246
119	0.0042	0.4199	47.5367
201	0.0044	0.4399	47.1325
207	0.0044	0.4409	46.9827
214	0.0042	0.4153	47.6328
231	0.0045	0.4535	44.6869

Table 4.5: FrST based denoising without added noise with  $a=0.5$ ,  $p=0.511$ ,  $q=0.51$

- For record 207 with noise, it is observed that with rotation factor  $a = 0.3$ , SNR is 44.52 dB, with  $a = 0.4$  SNR is 43.27 dB, with  $a = 0.5$  SNR is 41.24 dB and for  $a = 0.6$  SNR is 35.95 dB is obtained. It clearly shows that lesser is the value of rotation factor more good results are obtained.
- RMSE and hence PRD(%) is different for same records depending up the value of rotation factor.

Comparison between Overall performance of both the methods is shown in Figure 4.12. Figure 4.12 shows a bar graph between PRD(%) and the record numbers. It can be clearly seen that proposed method gives low value of PRD(%) implying lesser RMSE from the relation in (4.3). This shows that proposed method is superior than the ST method.

Record	RMSE	PRD	SNR
100	0.0087	0.8665	41.2444
101	0.0087	0.8689	41.2208
102	0.0091	0.9085	40.8334
103	0.0084	0.8403	41.5114
113	0.0082	0.8177	41.7485
119	0.0084	0.8414	41.4999
201	0.0085	0.8526	41.3847
207	0.0086	0.8665	41.2442
214	0.0084	0.8407	41.5067
217	0.009	0.8982	40.9323
231	0.0086	0.8574	41.3367

Table 4.6: FrST based denoising with added noise with  $a=0.5$ ,  $p=0.511$ ,  $q=0.51$

Record	RMSE	PRD	SNR
100	0.0143	1.4324	36.8786
101	0.0133	1.335	37.4907
102	0.0135	1.3493	37.3978
103	0.0127	1.2674	37.9421
113	0.0118	1.1787	38.5721
119	0.0114	1.1436	38.8348
201	0.0143	1.4328	36.876
207	0.0146	1.4598	36.714
214	0.0125	1.2459	38.0902
217	0.0116	1.161	38.7031
231	0.0131	1.3076	37.7

Table 4.7: FrST based denoising without added noise with  $a=0.6$ ,  $p=0.511$ ,  $q=0.51$

## 4.5 QRS Detection using T-F method

According to the medical definition, the most important information about ECG signal is almost concentrated in P-wave, QRS complex and T-wave. Also, QRS detection is the first step for all the kinds of automatic feature extraction. Therefore accurate detection of QRS [25] is an important task for many clinical conditions. Due to its characteristic shape, it serves as the basis for the automated determination of the heart beat rate, and for classification of the cardiac disease. Hence QRS detection is a crucial step in diagnosing human heart.

- **Conventional QRS Detection Techniques**

Record	RMSE	PRD	SNR
100	0.0162	1.622	35.7988
101	0.0154	1.5436	36.2291
102	0.0156	1.5581	36.1483
103	0.015	1.4953	36.5057
113	0.0144	1.4388	36.84
119	0.0139	1.3897	37.1418
201	0.016	1.6045	35.893
207	0.01529	1.5927	35.9571
214	0.0147	1.4665	36.6741
217	0.0154	1.5386	36.2575
231	0.015	1.5018	36.468

Table 4.8: FrST based denoising with added noise with  $a=0.6$ ,  $p=0.511$ ,  $q=0.51$

Record	RMSE	PRD	SNR
100	0.0016	0.1554	56.1711
101	0.0014	0.1357	57.3503
102	0.0019	0.19	54.4263
103	0.0012	0.1248	58.075
113	0.0019	0.1899	54.4304
119	0.0023	0.2303	52.7549
201	0.0015	0.1503	56.4594
207	0.0011	0.1119	59.0213
214	0.0019	0.1909	54.384
<b>217</b>	<b>0.0011</b>	<b>0.109</b>	<b>59.2549</b>
231	0.0016	0.156	56.1353

Table 4.9: FrST based denoising without added noise with  $a=0.3$ ,  $p=0.511$ ,  $q=0.51$

1. Template Matching Techniques: The basic idea behind this approach is the similarity between pattern, which is related to human cognitive process. Template Cross Correlation Method and Template Subtraction are the two methods [28]. A measure of similarity is provided by correlational coefficient in Template Cross Correlational Method. In other method, subtraction of each part of segment is performed from the segment presumed to be the QRS segment. The difference is close to zero when incoming ECG signal is aligned with the template.
2. Differentiation based QRS Detection Techniques: QRS complex has high frequency content therefore, differentiation [30] of QRS complex magnifies those high frequencies and attenuates other low frequencies of P and T. This method is exploited in two methods. First is based on simple principle of finding the width of QRS [19].

Record	RMSE	PRD	SNR
100	0.0061	0.6101	44.2924
101	0.0061	0.611	44.2797
102	0.0062	0.6242	44.094
103	0.0061	0.6142	44.2345
113	0.0064	0.6439	43.8235
119	0.0065	0.6484	43.7631
<b>201</b>	<b>0.006</b>	<b>0.6034</b>	<b>44.3885</b>
207	0.0059	0.5939	44.5252
214	0.0062	0.6197	44.1562
217	0.006	0.5984	44.4601
231	0.0061	0.6141	44.2346

Table 4.10: FrST based denoising with added noise with  $a=0.3$ ,  $p=0.511$ ,  $q=0.51$

Second one recognizes QRS complex based on analyses of the slope, amplitude and the width.

3. Pan-Tompkins algorithm: This algorithm is based on the 3 parameters; slope, amplitude and width of the signal. It is divided in two different stages: preprocessing and decision. In the preprocessing stage [26] the signal is prepared for later detection, removing the noise, smoothing the signal and amplifying the QRS slope and width. Different stages involved are : low pass filtering, high pass filtering, bandpass filtering, derivative based filtering, square filtering, moving average based filtering and adaptive threshold for the detection of QRS complex. In decision stage, thresholds are applied to the signal in order to remove noise peaks.

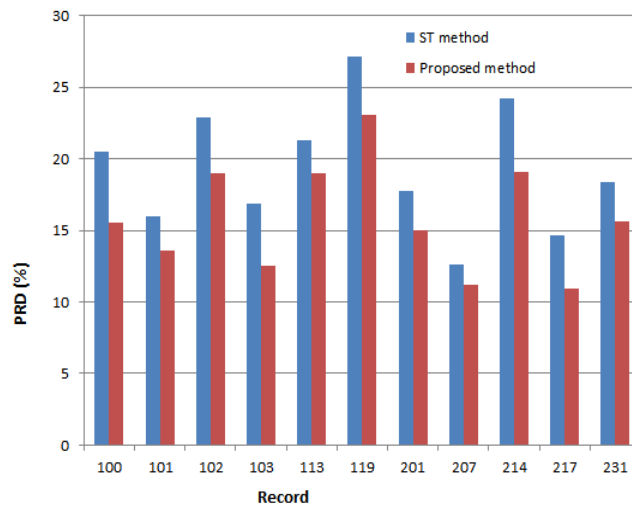


Figure 4.12: Comparison of the PRD(%) using different denoising methods

### 4.5.1 Concept of Shannon energy and QRS localization

Localizing [24] the QRS complexes is a crucial step in analyzing small transient changes in instant heart rate. It is directly linked with finding R-peaks. As ECG is a bipolar signal, it needs to be transformed into a unipolar signal. So methods used to achieve such unipolar signal are [22]:

1. Absolute value:  $y[n] = |a[n]|$
2. Squared value:  $y[n] = |a[n]| \times |a[n]|$
3. Shannon entropy value:  $y[n] = -|a[n]| \times \ln(|a[n]|)$
4. Shannon energy value:  $y[n] = -|a[n]|^2 \times \ln(a[n]^2)$

where  $a[n]$ ,  $|y[n]|$  are input and output for the above equations respectively.

The advantage of using Shannon energy instead of squared energy is that in case of significant change in amplitude of QRS, medium and low QRSs are better localised with Shannon than for the classical squared energy as shown in Fig4.13.

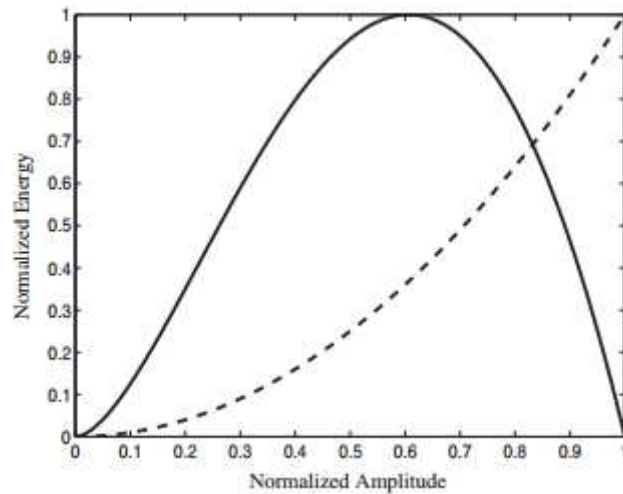


Figure 4.13: Normalized energy values with Shannon energy (solid) and squared energy (dashed)[21].

Shannon energy (SSE) exhibits a smooth envelope, completely removing the

effect of P and T waves. Its maxima coincides with the position of R-peaks. Therefore, this  $SSE$  of the signal can be retained as a temporal detection parameter.  $SSE$  for ECG signal can be computed by the following relation [31]:

1. SSE is calculated of the spectrum obtained for each sample( $j$ ) of the ECG signal by the formula,

$$SSE(j) = - \sum_{n=n_o}^{n_1} [S(j, n)]^2 \log [S(j, n)]^2 \quad (4.4)$$

where  $n_o$  and  $n_1$  corresponds to  $f_o=5$  Hz and  $f_1=22.5$  Hz.

2. Normalized Shannon energy is expressed as:

$$SSE_n = \frac{SSE}{|\max(SSE)|} \quad (4.5)$$

## 4.5.2 QRS detection using ST

Steps involved in QRS detection using ST are as follows [23]:

1. Calculation of ST of ECG signal.
2. Normalized Shannon energy  $SSE_n$  is computed.
3. QRS localisation: Threshold is applied on selected  $SSE_n$  associated with each sample  $j$  using  $\lambda = 0.3 * \max(SSE_n)$ .  
- if  $SSE_n(j) \geq \lambda$  then position  $j \in \text{QRS}$  - else  $j \notin \text{QRS}$ .
4. Identification of different QRS complexes by applying the constraint that, there should be difference of atleast  $36ms$  between the detected positions of QRS complex.
5. Elimination of multiple detection: As QRS cannot occur in refractory period ( $200ms$ ) therefore, a peak occurring in that interval is discarded.
6. Searchback is done for missed QRS complexes.

## 4.5.3 QRS detection using FrST

Steps involved in QRS detection using FrST are as follows:

1. FrST of the records is calculated.
2. Normalized Shannon energy  $SSE_n$  is computed using the (4.5).
3. For performing QRS localisation using FrST, same step 3 of Section 4.5.2 is followed.
4. Identification of different QRS complexes: Again the constraint is applied for positions which are at distance of less than  $36ms$ .
5. Elimination of multiple detection: As QRS cannot occur in refractory period ( $200ms$ ) therefore, a peak occurring in that interval is discarded.
6. Searchback is done for detecting missed QRS complexes.

#### 4.5.4 Results and Discussion

QRS detection is done using the proposed algorithm, using MITDB which contains 48 half-hours recordings of annotated ECG. Algorithm is applied on data length of  $10s$  which is sampled with rate  $360Hz$ . It is observed that some records are very highly corrupted with noise and artifacts, and had abnormal shape (e.g., records 108 and 207) and some contained clear R-peaks with less artifacts (e.g., records 100-107). Lead 1 is selected as QRS complex is more prominent in this lead than any other.

- Figure 4.14 and Figure 4.15 shows segment of record 214. 12 beats are present in first 10 seconds. Both the methods correctly detect the R-peaks.
- Figure 4.16 and Figure 4.17 shows segment of record 117. 9 beats are present and both the methods detect the peaks accurately but ST method fails to detect the QRS complex as the detected portion is not localised.
- Figure 4.18 and Figure 4.19 shows the segment of record 208. Total 16 beats are present, but ST detects only 10 beats. 6 undetected beats are left with the ST method. Threshold selected for ST was changed to detect those 10 beats correctly. FrST method correctly detects 16 beats with threshold level set at  $\lambda = 0.3max(SSE_n)$ .

The accuracy of our QRS detection algorithm was assessed by the use of statistical parameters defined as:

1. Sensitivity - Parameter which defines the ability of method used for detecting true

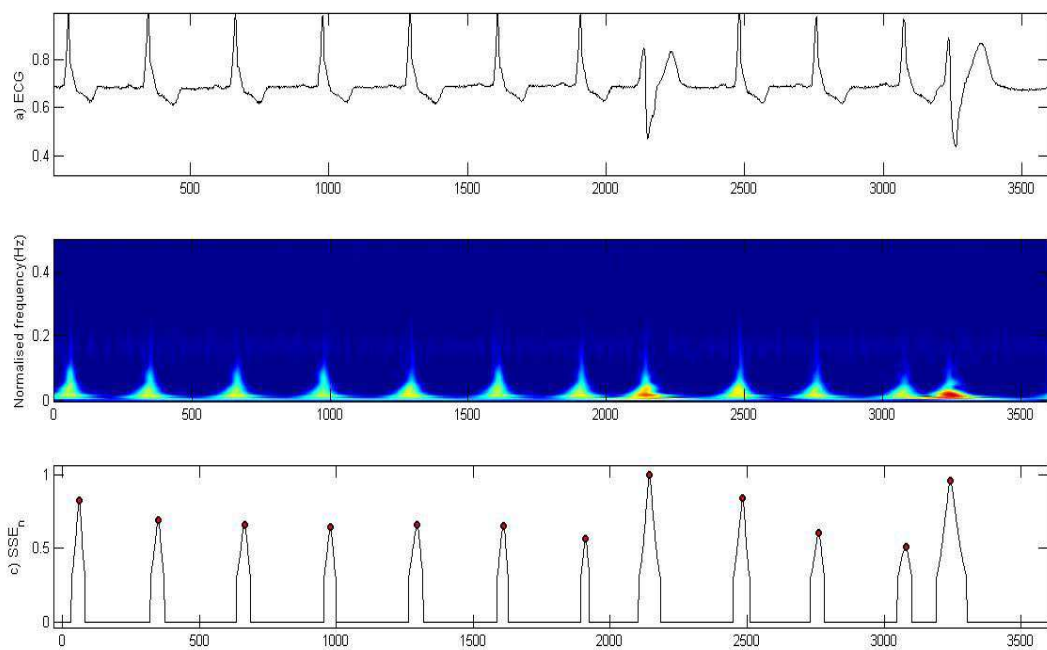


Figure 4.14: a) ECG-214 b)ST spectrum c) Shannon energy plot

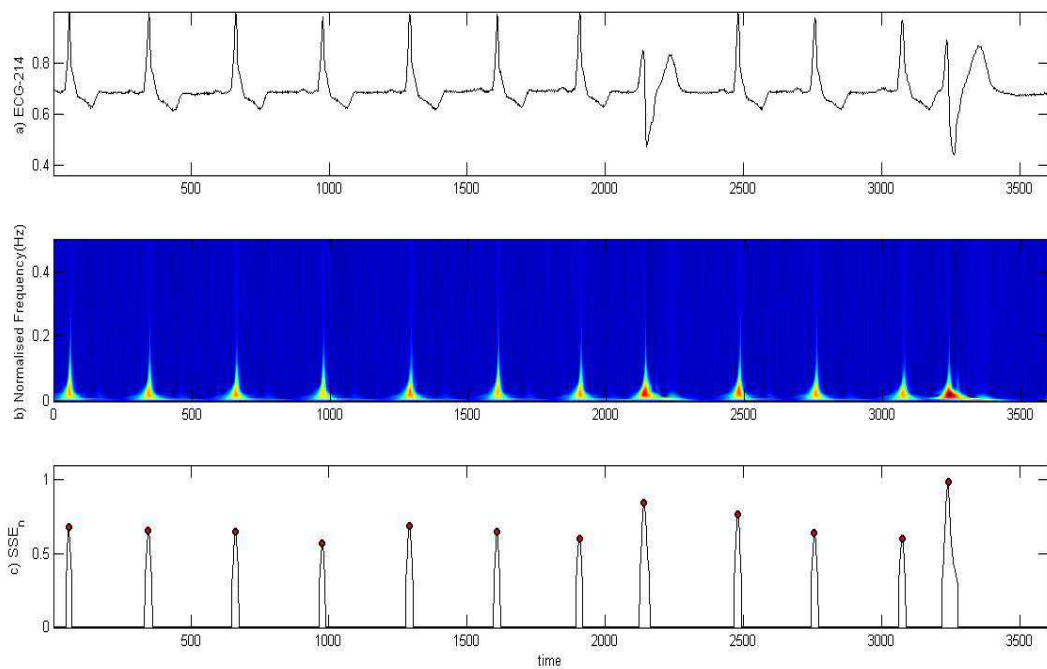


Figure 4.15: a) ECG-214 b) FrST spectrum c) Shannon energy plot

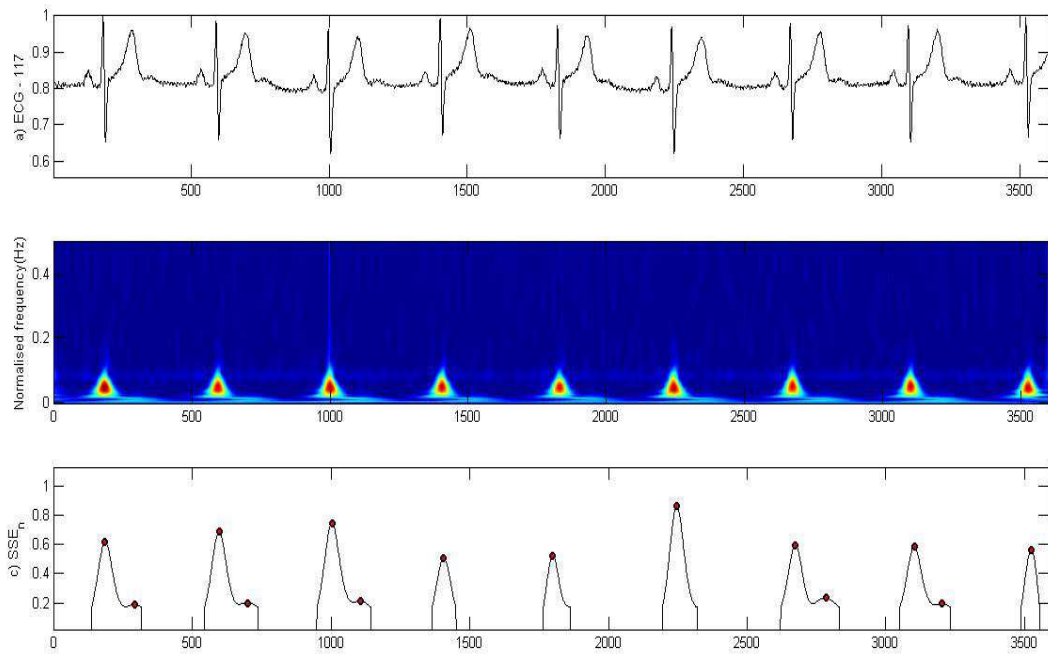


Figure 4.16: a) ECG-117 b) ST spectrum c) Shannon energy plot

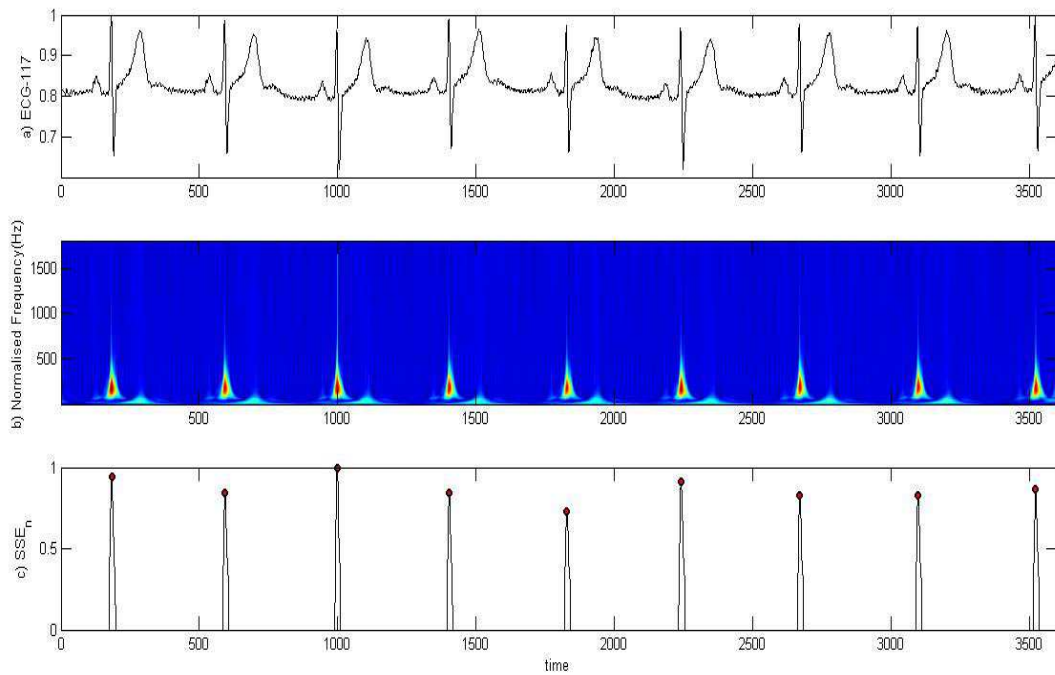


Figure 4.17: a) ECG-117 b) FrST spectrum c) Shannon energy plot

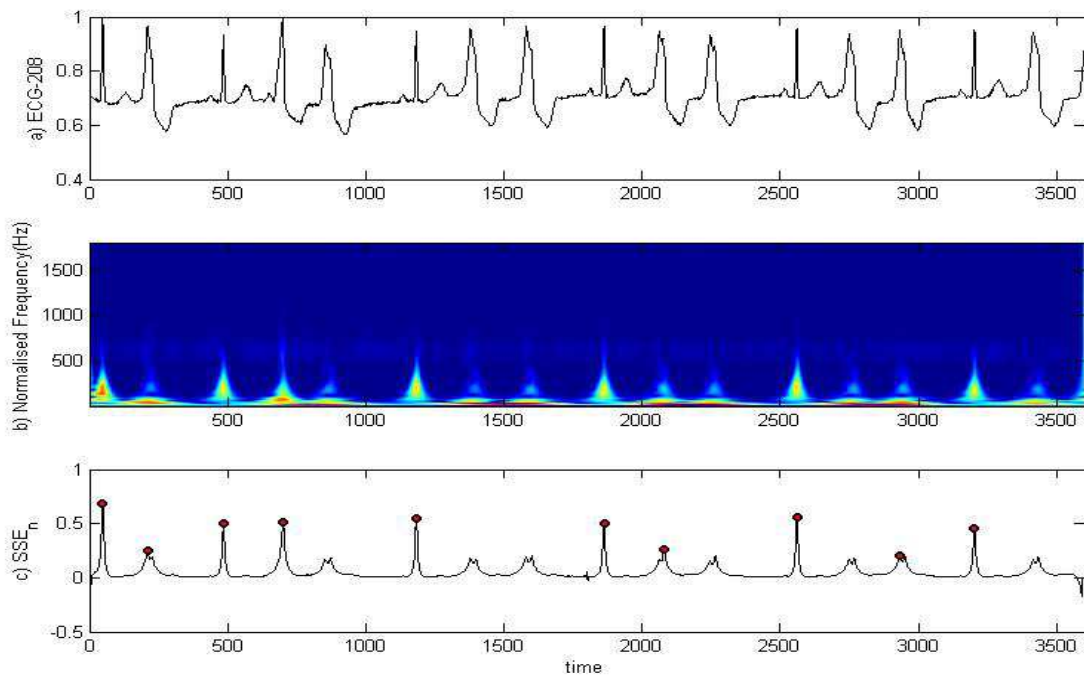


Figure 4.18: a) ECG-208 b) ST spectrum c) Shannon energy plot

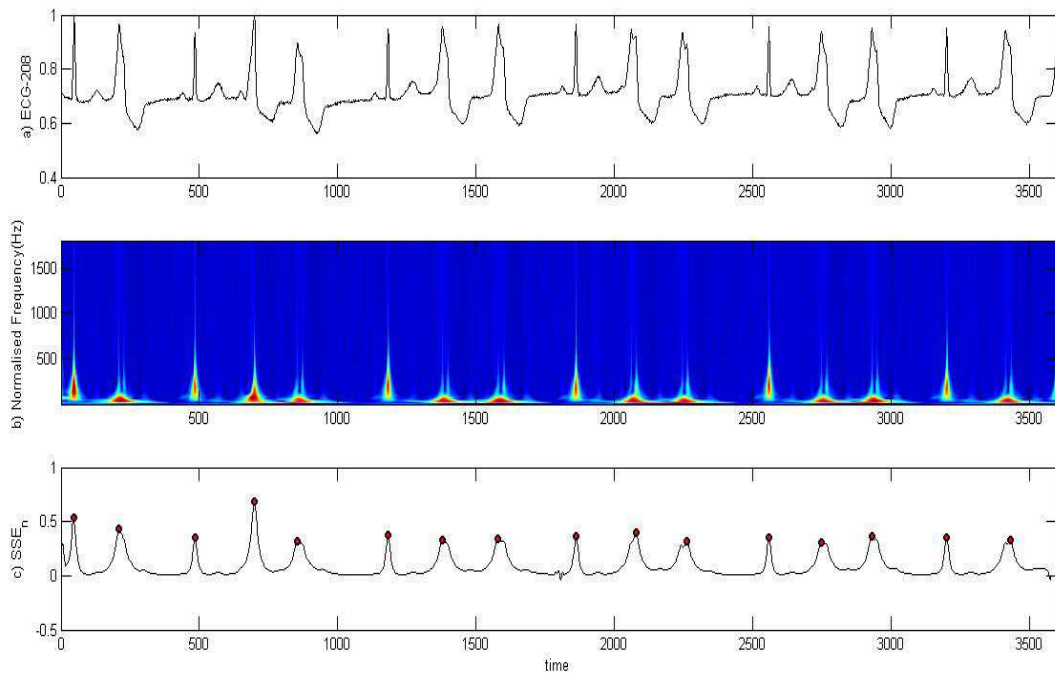


Figure 4.19: a) ECG-208 b) FrST spectrum c) Shannon energy plot

beats.

$$S_e = \frac{TP}{TP + FN} \quad (4.6)$$

2. Positive predictivity - Parameter for evaluating the ability of algorithm to differentiate between TP and FN.

$$P_+ = \frac{TP}{TP + FP} \quad (4.7)$$

3. Error rate - For evaluating the accuracy of algorithm.

$$E_r = \frac{FN + FP}{TP} \quad (4.8)$$

where TP is true positives, FP is false positives and FN is false negatives. According to decision making rule, a detection is a true beat if the detected R-peak lies within  $50ms$  otherwise the detection is false. The analysis of simulations result confirms that the both the methods can identify the R-peak position with reasonable accuracy. Achieved results reported in Table 4.13 and Table 4.12 proves that our algorithm succeeded by detecting correctly 98.37% of total beats. Also positive predictivity came out to be 99.83% and error rate of 1.82% is achieved. Comparison between the two methods is shown.

Method	Se(%)	P+(%)	Er(%)
Proposed Method	98.37	99.83	1.82
ST method	95.34	95.033	10.1

Table 4.11: Comparison of the algorithms

Rec	TP	FP	FN	Se(%)	P+ (%)	Er(%)
100	13	0	0	100	100	0
101	11	0	0	100	100	0
102	11	2	1	91.66	84.61	0.27
103	11	0	1	91.66	100	0.09
104	11	0	2	84.61	100	0.18
105	14	0	0	100	100	0
106	9	0	1	90	100	0.11
107	11	1	0	100	91.66	0.09
108	7	7	3	70	50	1.42
109	17	1	0	100	94.44	0.05
111	12	0	0	100	100	0
112	14	0	0	100	100	0
113	9	0	0	100	100	0
114	9	0	0	100	100	0
115	10	0	0	100	100	0
116	14	0	0	100	100	0
117	9	0	0	100	100	0
118	12	0	0	100	100	0
119	10	0	0	100	100	0
121	10	0	0	100	100	0
122	15	0	0	100	100	0
123	8	0	0	100	100	0
124	8	0	0	100	100	0
200	7	1	8	46.66	87.5	1.28
201	14	0	0	100	100	0
202	9	0	0	100	100	0
203	23	5	1	95.83	82.14	0.26
205	14	1	1	93.33	93.33	0.14
207	5	7	0	100	41.66	1.4
208	10	0	6	62.5	100	0.6
209	15	0	0	100	100	0
210	15	1	1	93.75	93.75	0.13
212	15	0	0	100	100	0
213	18	0	0	100	100	0
214	12	0	0	100	100	0
215	18	0	0	100	100	0
217	12	0	0	100	100	0
219	13	0	0	100	100	0
220	12	0	0	100	100	0
221	11	2	2	84.61	84.61	0.36
222	13	0	0	100	100	0
223	13	0	0	100	100	0
228	12	0	0	100	100	0
230	14	0	0	100	100	0
231	10	0	0	100	100	0
232	8	0	0	100	100	0
233	17	1	0	100	94.44	0.05
234	14	0	1	93.33	100	0.07

Table 4.12: Experimental results for QRS detection using ST

Rec	TP	FP	FN	Se(%)	P+ (%)	Er(%)
100	13	0	0	100	100	0
101	11	0	0	100	100	0
102	11	0	1	91.66	100	0.09
103	11	0	0	100	100	0
104	13	0	0	100	100	0
105	14	0	0	100	100	0
106	10	0	0	100	100	0
107	11	0	0	100	100	0
108	10	4	0	100	71.42	0.4
109	17	1	0	100	94.44	0.05
111	12	0	0	100	100	0
112	14	0	0	100	100	0
113	9	0	0	100	100	0
114	9	0	0	100	100	0
115	10	0	0	100	100	0
116	14	0	0	100	100	0
117	9	0	0	100	100	0
118	12	0	0	100	100	0
119	10	0	0	100	100	0
121	10	0	0	100	100	0
122	15	0	0	100	100	0
123	8	0	0	100	100	0
124	8	0	0	100	100	0
200	15	0	0	100	100	0
201	14	0	0	100	100	0
202	9	0	0	100	100	0
203	23	4	0	100	85.18	0.17
205	15	0	0	100	100	0
207	14	0	0	100	100	0
208	16	0	0	100	100	0
209	15	0	0	100	100	0
210	16	0	0	100	100	0
212	15	0	0	100	100	0
213	18	0	0	100	100	0
214	12	0	0	100	100	0
215	18	0	0	100	100	0
217	12	0	0	100	100	0
219	13	0	0	100	100	0
220	12	0	0	100	100	0
221	13	0	0	100	100	0
222	13	0	0	100	100	0
223	13	0	0	100	100	0
228	12	0	0	100	100	0
230	14	0	0	100	100	0
231	10	0	0	100	100	0
232	8	0	0	100	100	0
233	17	0	0	100	100	0
234	15	0	1	93.75	100	0.067

Table 4.13: Experimental results for QRS detection using FrST



# Chapter 5

## CONCLUSION AND FUTURE SCOPE OF WORK

### 5.1 Conclusion

This thesis examines non-stationary signals using JTFA tools. Out of various time-frequency methods ST is said to have better simultaneous resolution in time and frequency domains. It is observed that:

- The ST although has many advantages like multi-resolution analysis(MRA) and the absolute phase of frequency components of the signal but it degrades the time resolution at lower frequency and also gives poor frequency resolution at higher frequency. A modied Gaussian window was introduced which scales with the frequency and improves energy concentration of the ST. Therefore time-frequency localization problem was solved in a better way than for the standard ST.
- FrST is introduced for biomedical field in this thesis, which tends to show flexible nature for spectral analysis and superior time-frequency resolution providing better localisation.

Concept of JTFA in biomedical signal processing field basically focuses on ECG signals. Novel tool introduced for processing ECG signals proved to give much better results than time-frequency methods. Extended concept of ST in fractional fourier frequency domain achieved much greater filtering and denoising performance in processing ECG.

Resolving ability of FrST is established by changing the FrFT parameters which results in high flexibility for analysing ECG signal spectrum.

## 5.2 Future Scope

Study of JTFA is a topic beyond boundaries. It can be extended for exploring the biomedical field.

- FrST can be applied in analysing ECG signals for feature extraction and pattern recognition.
- Work can be done on reducing the computational complexity of FrST.
- FrST can be applied on EEG and on various other biomedical signals and also this concept can be used in image processing, as FrST is a very flexible transform and can enhance the spectrum analysis of non-stationary signals.

# References

- [1] Qian, S and Dapang C (1999). Joint time-frequency analysis, *IEEE Signal Processing Magazine*, 16(2), 52-67.
- [2] Stockwell RG (2007). A basis for efficient representation of the S-transform, *Digital Signal Processing*, 17(1), 371-393.
- [3] Boashash B, Time-frequency signal analysis and processing: a comprehensive reference, Amsterdam: Elsevier, 2003.
- [4] Cohen L (1994). The uncertainty principle in signal analysis, *Proceedings of the IEEE-SP International Symposium in Time-Frequency and Time-Scale Analysis*, pp. 182-185.
- [5] Ventosa S *et al.* (2008). The S-transform from a wavelet point of view, *IEEE Transactions on Signal Processing*, 56(7), 2771-2780.
- [6] Daubechies I (1996). Where do wavelets come from?- A personal point of view, *Proceedings of the IEEE*, 84(4), 510-513.
- [7] Sahu SS, Panda G, and George NV (2009). An improved S-transform for time-frequency analysis, *IEEE International In Advance Computing Conference(IACC)*, [9th: Patiala, India: 2009] pp. 315-319.
- [8] Rangayyan RM. *Biomedical Signal Analysis: A Case- Study Approach*, IEEE Press Series on Biomedical Engineering, 2002.
- [9] Stockwell RG, Mansinha L, and Lowe RP (1996). Localization of the complex spectrum: the S-transform, *IEEE Transactions on Signal Processing*, 44(4), 998-1001.
- [10] Ozaktas HM and Aytur o (1995). Fractional fourier domains, *Signal Processing*, 46(1),119-124.
- [11] Ping XD and Ke G (2012). Fractional S transform–Part 1: Theory. *Applied geophysics*, 9(1), pp.73.
- [12] Wang Y and Peng Z (2016). The optimal fractional S transform of seismic signal based on the normalized second-order central moment. *Journal of Applied Geophysics*, 129, pp.8-16.
- [13] Iaizzo PA. *Handbook of Cardiac Anatomy, Physiology, and Devices*, Springer Science

and *Business Media*, 2009.

[14] Chandrakar B, Yadav OP and Chandra VK (2013). A Survey of Noise Removal Techniques For ECG Signals, *International Journal of Advanced Research in Computer and Communication Engineering*, 2(3), 1354-1357.

[15] Mahamdy MA and Riley HB (2014). Performance Study of Different Denoising Methods for ECG Signals, *In Conference on Current and Future Trends of Information and Communication Technologies in Health care (ICTH)*, [4th : Nova Scotia, Canada: 2014] pp. 325-332.

[16] Sanyal A, Baral A and Lahiri A (2012). Application of S-transform for Removing Baseline Drift from ECG, *In national Computational Intelligence and Signal Processing (CISP)*, [2nd :Kolkata, India: 2012] pp. 153-157.

[17] Khaing AS and Naing ZM (2011). Quantitative Investigation of Digital Filters in Electrocardiogram with Simulated Noises, *International Journal of Information and Electronics Engineering*, 1(3), 210.

[18] Agrawal JP and R. Vijay R (2013). Time-Frequency Filtering with the S-transform Signals, *International Journal of Scientific and Research Publication*, 3(2), 1-5.

[19] Manikandan MS and Soman KP (2012). A novel method for detecting R-peaks in electrocardiogram (ECG) signal. *Biomedical Signal Processing and Control*, 7(2), 118-128.

[20] <https://www.physionet.org/cgi-bin/atm/ATM>.

[21] Zhu H and Dong J (2013). An R-peak detection method based on peaks of Shannon energy envelope. *Biomedical Signal Processing and Control*, 8(5), pp. 466-474.

[22] Fonseca P *et al.* (2014). A novel low-complexity post-processing algorithm for precise QRS localization. *Springer Plus*, 3(1), 376.

[23] Moukadem A *et al.* (2015). Stockwell transform optimization applied on the detection of split in heart sounds. *In Proceedings of the IEEE European Signal Processing Conference (EUSIPCO)*, [22nd : Lisbon, Portugal: 2015], 3(2), pp. 103-113. 2015-2019.

[24] Messaoud MB and Dr- Ing (2007). On the Algorithm for QRS Complexes Localisation in Electrocardiogram, *IJCSNS International Journal of Computer Science and Network Security*, 7(5), pp. 28-34.

[25] Chen SW, Chen HC, Chan HL (2006). A real-time QRS detection method based on

moving-averaging incorporating with wavelet denosing. *Computer Methods and Programs in Biomedicine*, 82(3), 187-195.

[26] Hamilton PS and Tompkins WJ (1986). Quantitative investigation of QRS detection rules using the MIT/BIH arrhythmia database, *IEEE Transaction on Biomedical Engineering*, 12(3), 1157-1165.

[27] Pan J and Tompkins WJ (1985). A real-time QRS detection algorithm, *IEEE Transactions on Biomedical Engineering*, 3(32), 230-236.

[28] Meyer C, Gavela JF and Harris M (2006). Combining algorithms in automatic detection of QRS complexes in ECG signals, *IEEE Transactions on Information Technology in Biomedicine*, 10(3), 468-475.

[29] Zidelmal Z *et al.* (2013). QRS detection based on wavelet coefficients, *Computer Methods and Programs in Biomedicine*, 107(3), 490-496.

[30] Arzeno NM, Deng ZD and Poon CS (2008). Analysis of First- Derivative Based QRS Detection Algorithms, *IEEE Transaction on Biomedical Engineering*, 55(2), 478-484.

[31] Zidelmal Z *et al.* (2014). QRS detection using S-Transform and Shannon energy, *Computer Methods and Programs in Biomedicine*, 116(1), 1-9.

[32] Alvarez RA, Penin AJM and Sobrino XAV (2015). Comparison of three QRS detection algorithms over public database, *In Conference on Enterprise Information Systems (CENTRIS)*, [2nd: Vilamoura,Portugal: 2015], 37(9), pp. 826-836.

[33] Rufas DC and Carrabina J (2015). Simple QRS detection with the MaMeMi filter, *Biomedical Signal Processing and Control*, 21(2), 137-145.

[34] Yeh YC, Wang WJ (2008). QRS complexes detection for ECG signal: The Difference Operation Method, *Computer Methods and Programs in Biomedicine*, 91(3), 245-254.